

**Spring 2023 – Epigenetics and Systems Biology**  
**Discussion Session (Epigenetics and Disease Etiology)**  
**Michael K. Skinner – Biol 476/576**  
**Week 13 (April 6)**

**Epigenetics and Disease Etiology**

Primary Papers

1. Godfrey, et al. (2007) *Pediatr Res.* 61(5 Pt 2):5R-10R. (PMID: 17413851)
2. Sun, et al. (2018) *Nature Medicine.* 24(9):1372-1383. (PMID: 29988127)
3. Garrido, et al (2021) *Clinical Epigenetics.* 13(1):6. (PMID: 33413568)

**Discussion**

Student 31 – Ref #1 above

- What is the mismatch concept?
- How does epigenetics apply to the hypothesis?
- What mechanism is involved in the developmental origins of disease?

Student 32 – Ref #2 above

- What preconception exposure was studied?
- What sperm epigenetic effect was observed?
- How was offspring metabolism altered?

Student 33 – Ref #3 above

- What was the experimental design and technology used?
- What EWAS epimutations were detected in sperm?
- What do the observations suggest regarding autism etiology and how it can be used?

# Epigenetic Mechanisms and the Mismatch Concept of the Developmental Origins of Health and Disease

KEITH M. GODFREY, KAREN A. LILLYCROP, GRAHAM C. BURDGE, PETER D. GLUCKMAN, AND MARK A. HANSON

*Centre for Developmental Origins of Health and Disease [K.M.G., K.A.L., G.C.B., M.A.H.], University of Southampton, Southampton SO16 5YA, United Kingdom; Liggins Institute and National Research Centre for Growth and Development [P.D.G.], University of Auckland, Private Bag 92019, Auckland, New Zealand*

**ABSTRACT:** There is now considerable evidence that elements of the heritable or familial component of disease susceptibility are transmitted by nongenomic means, and that environmental influences acting during early development shape disease risk in later life. The underlying mechanisms are thought to involve epigenetic modifications in nonimprinted genes induced by aspects of the developmental environment, which modify gene expression without altering DNA sequences. These changes result in life-long alterations in gene expression. Such nongenomic tuning of phenotype through developmental plasticity has adaptive value because it attempts to match an individual's responses to the environment predicted to be experienced. When the responses are mismatched, disease risk increases. An example of such mismatch is that arising either from inaccurate nutritional cues from the mother or placenta before birth, or from rapid environmental change through improved socioeconomic conditions, which contribute substantially to the increasing prevalence of type-2 diabetes, obesity, and cardiovascular disease. Recent evidence suggests that the effects can be transmitted to more than the immediately succeeding generation, through female and perhaps male lines. Future research into epigenetic processes may permit us to develop intervention strategies. (*Pediatr Res* 61: 5R–10R, 2007)

Epidemiologic studies have demonstrated a robust association between small size at birth and during infancy, and a greater risk of chronic disease including coronary heart disease, hypertension, stroke, type 2 diabetes, and osteoporosis in later life (1). It is now accepted that the associations do not reflect confounding by adult environmental risk factors such as smoking or socioeconomic status, and the original observations from the Southampton group have been extensively replicated worldwide (1). A recent meta-analysis of 18 studies reported that the relative risk of adult coronary heart disease was 0.84 for each 1 kg increase in birth weight (2). This value is likely to substantially underestimate the developmental influence as there is much experimental evidence that the prenatal environment can induce long-term cardiovascular effects without necessarily affecting size at birth (3). Moreover, profound effects have now been demonstrated if there is a “mismatch” between the early, developmental en-

vironment and the subsequent environment in childhood and adult life (4). These and other observations have resulted in wide recognition that the “Developmental Origins of Health and Disease” has major public health implications worldwide. For example, a recent World Health Organization Technical Consultation concluded, “The global burden of death, disability, and loss of human capital as a result of impaired fetal development is huge and affects both developed and developing countries” (5). The report advocates a move away from simply low birth weight, to broader considerations of maternal well-being, and achieving the optimal environment for the fetus to maximize its potential for a full and healthy life.

In parallel with the epidemiologic observations, animal studies have demonstrated the importance of epigenetic changes in mediating the effects on adult phenotype and physiology arising from perturbations of the developmental environment, including maternal diet (6,7), uterine blood flow (8), and maternal nursing behavior (9). The role of epigenetic processes in the early stages of some forms of cancer is well established (10), but we are only now starting to appreciate that epigenetic processes also have major implications for our understanding of evolutionary mechanisms and for human development, reproduction, and degenerative disease. The effects on the offspring of epigenetic changes during development in animals mimic aspects of human disease, for example, metabolic disease, impaired renal function, or exaggerated stress responses, and a coherent theory for a role of epigenetic mechanisms in the developmental origins of later chronic disease is emerging. This is the subject of this review.

## MISMATCH, DEVELOPMENTAL PLASTICITY, AND EPIGENETICS

Steep temporal trends in the incidence rates of cardiovascular disease in many populations suggest that the epidemiologic associations are unlikely to have arisen exclusively through the pleiotropic effects of genes that influence both fetal growth and later cardiovascular risk. In contrast, the effects are now viewed as the result of the phenotype estab-

Received November 14, 2006; accepted January 9, 2007.

Correspondence: Mark A. Hanson, Ph.D., Centre for Developmental Origins of Health and Disease, Princess Anne Hospital (Mailpoint 887), Coxford Road, Southampton SO16 5YA, UK; e-mail: m.hanson@soton.ac.uk

M.A.H. is supported by the British Heart Foundation.

DOI: 10.1203/pdr.0b013e318045bedb

**Abbreviations:** **Dnmt**, DNA methyltransferase; **CpG**, cytosine and guanine adjacent to each other in the genome, linked by a phosphodiester bond; **GR**, glucocorticoid receptor; **HDAC**, histone deacetylase; **HMT**, histone methyltransferase; **PPAR**, peroxisome proliferator-activated receptor; **RNS Pol**, RNA polymerase; **TF**, transcription factor

lished by the interaction between genes and the developmental environment using the processes of developmental plasticity (11–13). As in other species, developmental plasticity attempts to “tune” gene expression to produce a phenotype best suited to the predicted later environment (14). When the resulting phenotype is matched to its environment, the organism will remain healthy. When there is a mismatch, the individual’s ability to respond to environmental challenges may be inadequate and risk of disease increases. Thus, the degree of the mismatch determines the individual’s susceptibility to chronic disease (4).

The degree of mismatch can by definition be increased by either poorer environmental conditions during development, or richer conditions later, or both (4). Unbalanced maternal diet, body composition, or disease can perturb the former; the rapid increase in energy-dense foods and reduced physical activity levels associated with a western lifestyle will increase the degree of mismatch *via* the latter (Fig. 1). Such changes are of considerable importance in developing societies going through rapid socioeconomic transitions. In this review, we focus on the epigenetic components of such inherited risk of disease, while noting that other, nongenomic mechanisms also operate to alter risk of disease in subsequent generations, *e.g.* the passage of cultural risk factors such as smoking.

The processes of phenotypic induction through developmental plasticity produce integrated changes in a range of organs *via* epigenetic processes. They establish a life-course strategy for meeting the demands of the predicted later environment (15). This explains why an impaired early environment produces a range of effects—alterations in cardiovascular and metabolic homeostasis, growth and body composition, cognitive and behavioral development, reproductive function,

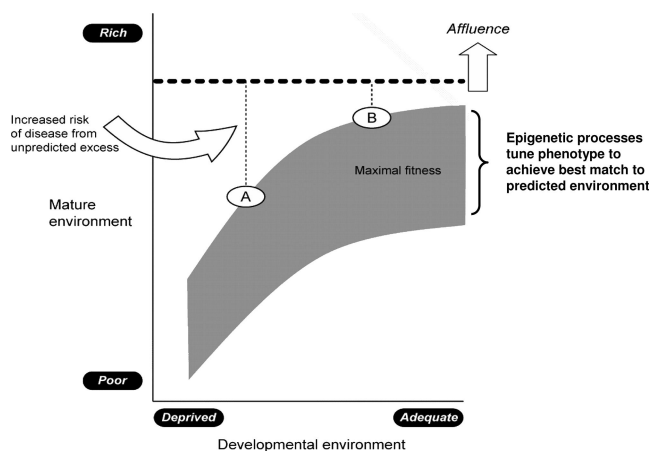


**Figure 1.** The mismatch concept emphasizes that the degree of disparity between the environment experienced during development and that experienced later influences the risk of disease. During the period of developmental plasticity in prenatal and early postnatal life, epigenetic processes are thought to alter gene expression to produce phenotypic attributes best suited to the environment in which the individual predicts that it will live, based on environmental cues transmitted *via* the mother. Greater mismatch gives greater risk of disease from unpredicted excessive richness (high calorie density food, sedentary lifestyle) of the environment. Thus, risk is greater with poorer developmental environment (A vs B), and with socioeconomic transitions to an affluent western lifestyle. Adapted from Gluckman PD *et al.* 2007 *Am J Hum Biol* 19:1–19 © 2006 Wiley-Liss, Inc., with permission.

repair processes and longevity—some of which are associated with increased risk of cardiovascular and metabolic disease, “precocious” puberty, osteoporosis, and some forms of cancer. Understanding the underlying epigenetic processes thus holds the key to understanding the underlying pathophysiology and to developing approaches to early diagnosis, prevention and treatment of these diseases.

## EPIGENETIC PROCESSES—DEFINITION AND MECHANISMS

The term “epigenetic” was coined by Waddington (16) to refer to the ways in which the developmental environment can influence the mature phenotype. His work and that of others (17) on developmental plasticity stemmed from observations that environmental influences during development could induce alternative phenotypes from a genotype, some of the clearest examples being polyphenisms in insects (18). Such processes can, however, also induce a gradation of phenotypes, constituting a population reaction norm (19). Waddington showed in *Drosophila melanogaster* that wing vein pattern could be affected by heat shock treatment of the pupae (20). Breeding individuals with these environmentally induced changes led eventually to a stable population exhibiting the phenotype without the environmental stimulus. Waddington termed this “genetic assimilation.” Such work, largely overlooked by proponents of the modern synthesis of genetic and evolutionary biology (21), demonstrates a dynamic interaction between the genome and the environment during the plastic phase of development, producing effects that can be heritable (11) in terms of an environmental cue acting in one generation having effects that are manifest in subsequent generations.

The term “epigenetic” is now used to refer to structural changes to genes that do not alter the nucleotide sequence, with epigenetic inheritance being defined as biologic processes that regulate mitotically or meiotically heritable changes in gene expression without altering the DNA sequence (22). Of particular relevance is methylation of specific CpG dinucleotides in gene promoters and alterations in DNA packaging arising from chemical modifications of the chromatin histone core around which DNA wraps (Fig. 2). The modifications include acetylation, methylation, ubiquitination, and phosphorylation. Such epigenetic inheritance systems (23) can be random with respect to the environment and have been termed “epimutations” (24), or specific epigenetic changes can be induced by the environment (25) (Fig. 3).

Epigenetic mechanisms are widely implicated in cancer (10). Promoter methylation is important for asymmetrical silencing of imprinted genes (26) and retrotransposons (27,28). However, they also play a critical role in a range of developmental processes. With the exception of imprinted genes, widespread removal of epigenetic marks occurs following fertilization when maternal and paternal genomes undergo extensive demethylation to ensure pluripotency of the developing zygote. This is followed by *de novo* methylation just before implantation (29,30). About 70% of CpGs are methylated, mainly in repressive heterochromatin regions and in repetitive sequences such as retrotransposable elements (31).

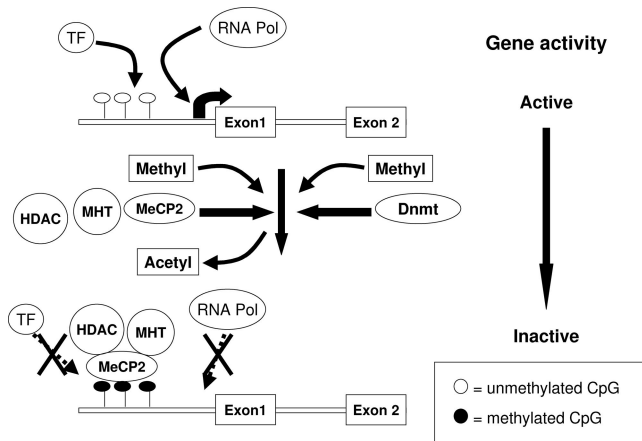


**Figure 2.** Epigenetic silencing of transcription. When CpG dinucleotides are unmethylated in the promoter, RNA Pol and TF can bind to specific nucleotide sequences and the coding region (exon) is transcribed. Methylation of CpGs by the activity of Dnmt enables recruitment of methyl CpG binding protein-2 (MeCP2), which in turn recruits HDAC/ HMT to form an enzyme complex bound to the gene promoter. The MeCP2/HDAC/HMT complex removes acetyl groups from histones and catalyses di- and tri- methylation of specific lysine residues which causes the DNA to condense. This prevents access of RNA polymerase and transcription factors to DNA and so converts transcriptionally active euchromatin to inactive heterochromatin. Thus, the overall effect of DNA and histone methylation is to induce long-term silencing of transcription.

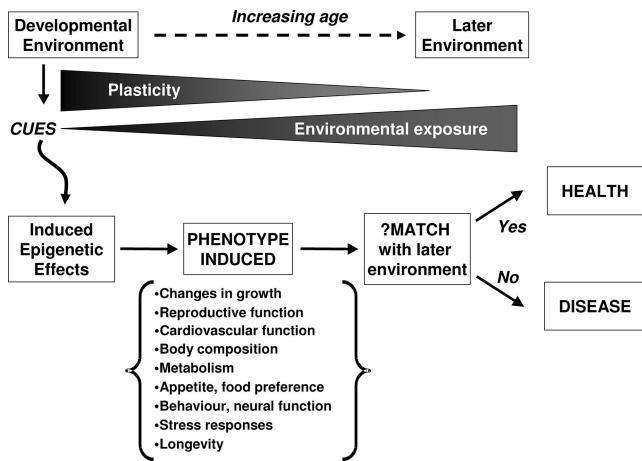


**Figure 3.** Developmental plasticity declines and exposure to environmental challenges increases with age. Epigenetic processes are induced by cues from the developmental environment. They play a role in determining the phenotype of the offspring as part of a life-course strategy to match it to its environment. If not appropriately matched, the risk of later disease is increased.

DNA methylation also plays a key role in cell differentiation by silencing the expression of specific genes during the development and differentiation of individual tissues. For example, the expression of the homeobox gene Oct-4, a key regulator of cellular pluripotency in the early embryo, is permanently silenced by hypermethylation of its promoter around E6.5 in the mouse (32), whereas HoxA5 and HoxB5, which are required for later stages of development, are not methylated and silenced until early postnatal life (33). For some genes there also appear to be gradations of promoter demethylation associated with developmental changes in role of the gene product. The  $\delta$ -crystallin II and phosphoenolpyruvate carboxykinase promoters are methylated in the early

embryo but undergo progressive demethylation during fetal development, and are hypomethylated compared with the embryo and expressed in the adult (34,35). Thus, changes in methylation that are associated with cell differentiation and functional changes are established at different times during development of the embryo. The pattern of DNA methylation is copied during mitosis by Dnmt-1 activity. This provides an “epigenetic memory” of patterns of gene regulation, and hence cell function, which is established during development and which is passed to the adult (29). This immediately suggests a mechanism by which the environment may induce stable changes to cell function that persist in the adult organism, by which environmental challenges at different times during development may produce different phenotypic outcomes and in humans differential risk of disease.

Genomic imprinting represents a special case of epigenetic regulation of genes (36). Through imprinting (which bears no relation to the term for behavioral conditioning defined by Lorenz), heritable patterns of gene expression are induced without changes in the sequence of genomic DNA through the silencing of one set of alleles dependent on its parental gender origin. Disease resulting from imprinting disorders is well recognized, e.g. Beckwith-Wiedemann syndrome. Although rare, the incidence of this disorder is increased in offspring conceived by assisted reproductive techniques (37). Imprinting is most frequently mediated by allele-specific DNA methylation, although imprinted alleles may differ in other ways.

Small noncoding regulatory RNA regulation of gene expression is a newly emerging epigenetic mechanism (25). These microRNAs have been shown to not only modulate the stability and translation of mRNAs, but also can induce gene silencing through the induction of gene methylation and alterations in chromatin structure. However, whether early life environmental challenges such as maternal nutritional constraints can alter the expression or formation of these microRNAs in the offspring has yet to be discovered, and the precise role that these microRNAs play in the developmental origins of adult disease remains to be determined.

**EVIDENCE FOR NONGENOMIC INHERITANCE IN HUMANS**

Human studies have provided a number of lines of evidence suggesting transgenerational nongenomic inheritance, although it is inevitably difficult to define the relative contributions of genetic, epigenetic, and common environmental or learned behavioral factors. For example, patterns of smoking, diet, and exercise can affect risk across more than one generation (38) by several mechanisms. Strong evidence for transgenerational nongenomic inheritance exists for dietary and endocrine exposures. Records from Överkalix in northern Sweden for individuals born in 1890, 1905, and 1920 have shown that diabetes mortality increased in men if the paternal grandfather was exposed to abundant nutrition during his prepubertal growth period (39), an effect later extended to paternal grandmother/granddaughter pairs and transmitted in a gender-specific fashion (40). During the 1944/1945 famine in the Netherlands, previously adequately nourished women



were subjected to low caloric intake and associated environmental stress. Pregnant women exposed to famine in late pregnancy gave birth to smaller babies (41) who had an increased risk of later insulin resistance (42). Famine exposure at different stages of gestation was variously associated with an increased risk of obesity, dyslipidemia, and coronary heart disease, and F2 offspring of females exposed in the first trimester *in utero* did not have the expected increase in birth weight with increasing birth order (41). Exposure of pregnant women to diethylstilbestrol led to a marked increase in reproductive abnormalities and uterine fibroids (43), an earlier menopause (44), and breast (45) and rare genital tract cancers in their children, and there is evidence of third-generational effects transmitted through the maternal line (46).

### EVIDENCE OF EPIGENETIC MECHANISMS IN ANIMALS

Animal research has given us new insights into developmental plasticity and epigenetics. First, it is clear that such epigenetic effects during development produce graded changes in the expression of a range of genes, in addition to those that produce parent-specific effects mediated *via* imprinted genes. Feeding a reduced protein diet to pregnant rats induces permanent changes in gene expression in the offspring; GR and PPAR $\alpha$  expression is increased in the liver (7,47), whereas expression of the enzyme that inactivates corticosteroids, 11 $\beta$ -hydroxysteroid dehydrogenase type II, is reduced in liver, lung, kidney, and brain (48). In the liver, increased GR and PPAR $\alpha$  expression is due to hypomethylation of their respective promoters (7). The PPAR $\alpha$  promoter is also hypomethylated in the heart (49). In contrast, there was no difference in methylation of the PPAR $\gamma$ 1 promoter in the liver, which suggests that the changes in epigenetic regulation induced by the maternal reduced protein diet were gene-specific (7). Graded silencing of the retrotransposon IAP element that regulates the agouti phenotype has been shown in the offspring of mice fed diets with different amounts of folic acid during pregnancy (6). Nondietary factors also induce altered epigenetic regulation of genes. Epigenetic changes in the methylation of renal p53 are produced by uterine blood flow restriction and are associated with reduced nephron number (8), which may precede the development of hypertension (50). Variations in maternal behavior also lead to epigenetic changes; in rats, maternal care of the pups influences methylation of the estrogen receptor- $\alpha$ 1b (51) and the hippocampal GR1 $_7$  promoters (9), the latter resulting in changes in hypothalamic-pituitary-adrenal axis stress responses (9). This study illustrates that epigenetic changes can be induced in later stages of developmental plasticity, such as during early postnatal life.

The levels of methylation of CpG bases in the genome are controlled in part by the activity of Dnmts. The developmental effects observed in the rat are not produced by changes in the expression of Dnmt-3a or b, or in the activity of methyl binding domain protein-2 (52), revealing that they are not produced by changes in the demethylation/remethylation processes that occur soon after fertilization (29,30). In contrast,

they are accompanied by decreased Dnmt-1 expression (52). This suggests a mechanism by which down-regulation of Dnmt-1 expression during early development leads to a progressive loss of epigenetic memory and an altered adult phenotype. This accords with the effects of nutritional or endocrine challenges during early gestation in altering growth of organs such as the heart and liver (53,54) and producing later effects on cardiovascular and metabolic control (55–57). In the rat, the epigenetic effects appear to be dependent on 1-carbon metabolism. Supplementation of the reduced protein diet with folic acid during pregnancy prevents cardiovascular changes in the offspring (58) and normalizes the changes in GR and PPAR $\alpha$  promoter methylation and gene expression (7) and in Dnmt-1 binding and expression (52). Induction of elevated blood pressure or endothelial dysfunction in the offspring is also prevented by maternal supplementation with glycine, but not with alanine or urea (59,60), supporting the concept that methyl group provision is important.

Furthermore, recent data show that both the effects of glucocorticoid treatment and the reduced protein diet in pregnancy can be passed to the second generation without further nutritional or endocrine manipulation (58,61,62). Feeding rats a reduced protein diet during pregnancy in the F0 generation induces hypomethylation of the PPAR $\alpha$  and GR promoters in the livers of both the F1 and F2 male offspring (62). This shows that transmission of induced phenotypes between generations involves altered epigenetic regulation of specific genes.

### ADAPTIVE VALUE OF NONGENOMIC INHERITANCE

The increasing evidence for nongenomic inheritance and particularly epigenetic inheritance raises the question of why the processes underpinning it have been preserved through evolution. Natural selection is generally viewed as a process by which a species and its environment become well matched. Developmental plasticity utilizes environmental cues to adjust individual phenotype to the current and predicted environment (13,63). These processes of developmental plasticity leading to nongenomic inheritance may have evolved to enhance fitness during shorter-term environmental shifts than Darwinian selection can necessarily cope with, and/or to ensure a greater match to a variable environment than selection alone can generate. In addition, it enables the induction of a wider range of phenotypes, permitting survival in a broader range of environments. Such strategies may have been important in the evolution of mammalian generalist species (64). Theoretical models demonstrate the circumstances under which fitness is enhanced if parents transmit information about the environment to their progeny. Factors to consider include the fidelity of the transmission of environmental cues, the degree of predictability of environmental conditions, and the costs of incorrect prediction (63,65–67).

### RELEVANCE OF EPIGENETIC PROCESSES TO THE RISK OF ADULT DISEASE

We now live much longer than our hominine ancestors. Thus, mechanisms selected for their advantage in our earlier

evolution may no longer be advantageous or may be advantageous in the young and disadvantageous in the elderly. There are limits to the environment that the fetus can sense and use to adjust its development (68). Nongenomic epigenetic processes of transmitting environmental information between generations evolved to assist our evolution as we moved across changing environments. They may also have served to buffer critical aspects of our development, especially the vulnerable period of weaning in infancy, against short-term environmental changes occurring between generations (69). Such processes were not designed to deal with the massive mismatch between the generally constrained fetal environment and the modern postnatal environment of high-energy intake and low energy expenditure (4) and disease risk is amplified by a greater mismatch between the prenatally predicted and actual adult environments. As a result, societies in rapid economic transition are particularly vulnerable (70–73). Epigenetic and other nongenomic inheritance processes may have conferred survival advantage on evolving hominids; they now exacerbate risk of disease for several successive generations and play a major part in the current epidemics of metabolic and cardiovascular disease (14,73). Additionally, the possibility is now being explored that exposure to xenobiotics such as endocrine disruptors may have multigenerational effects through female and male lines by actions on similar epigenetic mechanisms (74).

Lastly, returning to our starting point of population studies, we must note that there is increasing evidence for the effects of maternal obesity and gestational diabetes as risk factors for later metabolic and cardiovascular disease in the offspring (75,76), a concept again supported by experimental studies in animals (77). These effects contribute to the increasing transgenerationally passed rising incidence of such disease in both developed and developing societies. The extent to which such risk of disease operates by epigenetic processes is not known.

## CONCLUSION

Epigenetic changes provide a “memory” of developmental plastic responses to early environment. Their effects may only become manifest later in life, *e.g.* in terms of altered responses to environmental challenges. If the epigenetic change has occurred in part of the genome where gene expression is controlled by a transcription factor, then the consequences of the change will not become manifest until the transcription factor operates. There is additional potential for epigenetic marks to change throughout life as shown by recent studies on homozygous twins (78), and there is some evidence for inheritance of tissue-specific DNA methylation patterns (79). It is now important to conduct further research to determine the specific role of epigenetic processes in the development of risk of cardiovascular and metabolic disease or other sequelae.

**Acknowledgments.** The authors thank Dr. Alan Beedle for his assistance with the literature search and editing of the manuscript.

## REFERENCES

- Godfrey KM 2006 The “Developmental Origins” hypothesis: epidemiology. In: Gluckman PD, Hanson MA (eds) *Developmental Origins of Health and Disease—A Biomedical Perspective*. Cambridge University Press, pp 6–32
- Huxley R, Owen C, Whincup P, Cook D, Rich-Edwards J, Smith G 2007 Is birthweight a risk factor for coronary heart disease in later life? *J Epidemiol* (in press)
- Hanson MA, Gluckman PD 2005 Developmental processes and the induction of cardiovascular function: conceptual aspects. *J Physiol* 565:27–34
- Gluckman PD, Hanson MA 2006 *Mismatch; How Our World No Longer Fits Our Bodies*. Oxford University Press, Oxford
- Promoting Optimal Fetal Development: Report of a Technical Consultation. World Health Organization. Available at: [http://www.who.int/nutrition/topics/fetal\\_dev\\_report\\_EN.pdf](http://www.who.int/nutrition/topics/fetal_dev_report_EN.pdf)
- Waterland RA, Jirtle RL 2003 Transposable elements: targets for early nutritional effects on epigenetic gene regulation. *Mol Cell Biol* 23:5293–5300
- Lillycrop KA, Phillips ES, Jackson AA, Hanson MA, Burdge GC 2005 Dietary protein restriction of pregnant rats induces and folic acid supplementation prevents epigenetic modification of hepatic gene expression in the offspring. *J Nutr* 135:1382–1386
- Pham TD, MacLennan NK, Chiu CT, Laksana GS, Hsu JL, Lane RH 2003 Uteroplacental insufficiency increases apoptosis and alters p53 gene methylation in the full-term IUGR rat kidney. *Am J Physiol Regul Integr Comp Physiol* 285:R962–R970
- Weaver IC, Cervoni N, Champagne FA, D’Alessio AC, Sharma S, Seckl JR, Dymov S, Szyf M, Meaney MJ 2004 Epigenetic programming by maternal behavior. *Nat Neurosci* 7:847–854
- Laird PW 2005 Cancer epigenetics. *Hum Mol Genet* 14:R65–R76
- West-Eberhard MJ 2003 *Developmental Plasticity and Evolution*. Oxford University Press, New York
- Bateson P, Barker D, Clutton-Brock T, Deb D, Foley RA, Gluckman P, Godfrey K, Kirkwood T, Mirazon Lahr M, Macnamara J, Metcalfe NB, Monaghan P, Spencer HG, Sultan SE 2004 Developmental plasticity and human health. *Nature* 430:419–421
- Gluckman PD, Hanson MA, Spencer HG, Bateson P 2005 Environmental influences during development and their later consequences for health and disease: implications for the interpretation of empirical studies. *Proc Biol Sci* 272:671–677
- Gluckman PD, Hanson MA 2004 Living with the past: evolution, development and patterns of disease. *Science* 305:1733–1736
- Gluckman PD, Hanson MA, Beedle AS 2007 Early life events and their consequences for later disease; a life history and evolutionary perspective. *Am J Hum Biol* 19:1–19
- Van Speybroeck L 2002 From epigenesis to epigenetics. The case of C.H. Waddington. *Ann N Y Acad Sci* 981:61–81
- Schmalhausen I 1949 *Factors of Evolution; the Theory of Stabilizing Selection*. Blakiston, McGraw-Hill, New York
- Applebaum SW, Heifetz Y 1999 Density-dependent physiological phase in insects. *Annu Rev Entomol* 44:317–341
- Schlichting CD, Pigliucci M 1998 Phenotypic evolution: a reaction norm perspective. Sinauer Associates Inc., Sunderland, MA
- Waddington CH 1957 *The Strategy of the Genes: A Discussion of Some Aspects of Theoretical Biology*. Macmillan, New York
- Mayr E 2001 *What Evolution Is*. Basic Books, New York
- Jablonka E, Lamb MJ 2005 *Evolution in Four Dimensions: Genetic, Epigenetic, Behavioral and Symbolic Variation in the History of Life*. MIT Press, Cambridge, MA
- Maynard Smith J 1990 Models of a Dual Inheritance System. *J Theor Biol* 143:41–53.
- Holliday R 1991 Mutations and Epimutations in Mammalian Cells. *Mutat Res* 250:351–363
- Gluckman PD, Hanson MA, Beedle AS 2007 Non-genomic transgenerational inheritance of disease risk. *Bioessays* 29:145–154
- Li E, Beard C, Jaenisch R 1993 Role for DNA methylation in genomic imprinting. *Nature* 366:362–365
- Walsh CP, Chaillet JR, Bestor TH 1998 Transcription of IAP endogenous retroviruses is constrained by cytosine methylation. *Nat Genet* 20:116–117
- Waterland RA, Jirtle RL 2003 Transposable elements: targets for early nutritional effects on epigenetic gene regulation. *Mol Cell Biol* 23:5293–5300
- Bird A 2002 DNA methylation patterns and epigenetic memory. *Genes Dev* 16:6–21
- Reik W, Dean W, Walter J 2001 Epigenetic reprogramming in mammalian development. *Science* 293:1089–1093
- Yoder JA, Soman NS, Verdine GL, Bestor TH 1997 DNA (cytosine-5)-methyltransferases in mouse cells and tissues. Studies with a mechanism-based probe. *J Mol Biol* 270:385–395
- Gidekel S, Bergman Y 2002 A unique developmental pattern of Oct-3/4 DNA methylation is controlled by a cis-demodification element. *J Biol Chem* 277:34521–34530
- Hershko AY, Kafri T, Fainsod A, Razin A 2003 Methylation of HoxA5 and HoxB5 and its relevance to expression during mouse development. *Gene* 302:65–72
- Grainger RM, Hazard-Leonards RM, Samaha F, Hougan LM, Lesk MR, Thomsen GH 1983 Is hypomethylation linked to activation of delta-crystallin genes during lens development? *Nature* 306:88–91
- Benvenisty N, Mencher D, Meyuhos O, Razin A, Reshef L 1985 Sequential changes in DNA methylation patterns of the rat phosphoenolpyruvate carboxykinase gene during development. *Proc Natl Acad Sci U S A* 82:267–271

36. Reik W, Walter J 2001 Genomic imprinting: parental influence on the genome. *Nat Rev Genet* 2:21–32
37. Arnaud P, Feil R 2005 Epigenetic deregulation of genomic imprinting in human disorders and following assisted reproduction. *Birth Defects Res C Embryo Today* 75:81–97
38. Brook JS, Whiteman M, Brook DW 1999 Transmission of risk factors across three generations. *Psychol Rep* 85:227–241
39. Kaati G, Bygren LO, Edvinsson S 2002 Cardiovascular and diabetes mortality determined by nutrition during parents' and grandparents' slow growth period. *Eur J Hum Genet* 10:682–688
40. Pembrey ME, Bygren LO, Kaati G, Edvinsson S, Northstone K, Sjöström M, Golding J, ALSPAC Study Team 2006 Sex-specific, male-line transgenerational responses in humans. *Eur J Hum Genet* 14:159–166
41. Lumey LH, Stein AD 1997 Offspring birth weights after maternal intrauterine undernutrition: a comparison within sibships. *Am J Epidemiol* 146:810–819
42. Painter RC, Roseboom TJ, Bleker OP 2005 Prenatal exposure to the Dutch famine and disease in later life: an overview. *Reprod Toxicol* 20:345–352
43. Baird DD, Newbold R 2005 Prenatal diethylstilbestrol (DES) exposure is associated with uterine leiomyoma development. *Reprod Toxicol* 20:81–84
44. Hatch EE, Troisi R, Wise LA, Hyer M, Palmer JR, Titus-Ernstoff L, Strohsnitter W, Kaufman R, Adam E, Noller KL, Herbst AL, Robboy S, Hartge P, Hoover RN 2006 Age at natural menopause in women exposed to diethylstilbestrol *in utero*. *Am J Epidemiol* 164:682–688
45. Palmer JR, Wise LA, Hatch EE, Troisi R, Titus-Ernstoff L, Strohsnitter W, Kaufman R, Herbst AL, Noller KL, Hyer M, Hoover RN 2006 Prenatal diethylstilbestrol exposure and risk of breast cancer. *Cancer Epidemiol Biomarkers Prev* 15:1509–1514
46. Brouwers MM, Feitz WF, Roelofs LA, Kiemeny LA, de Gier RP, Roeleveld N 2006 Hypospadias: a transgenerational effect of diethylstilbestrol? *Hum Reprod* 21:666–669
47. Burdge GC, Phillips ES, Dunn RL, Jackson AA, Lillycrop KA 2004 Effect of reduced maternal protein consumption during pregnancy in the rat on plasma lipid concentrations and expression of peroxisomal proliferator-activated receptors in the liver and adipose tissue of the offspring. *Nutr Res* 24:639–646
48. Bertram C, Trowern AR, Copin N, Jackson AA, Whorwood CB 2001 The maternal diet during pregnancy programs altered expression of the glucocorticoid receptor and type 2 11beta-hydroxysteroid dehydrogenase: potential molecular mechanisms underlying the programming of hypertension *in utero*. *Endocrinology* 142:2841–2853
49. Burdge GC, Hanson MA, Slater-Jefferies JL, Lillycrop KA 2007 Epigenetic regulation of transcription: a mechanism for inducing variations in phenotype (fetal programming) by differences in nutrition during early life? *Br J Nutr* (in press)
50. Woods LL, Ingelfinger JR, Nyengaard JR, Rasch R 2001 Maternal protein restriction suppresses the newborn renin-angiotensin system and programs adult hypertension in rats. *Pediatr Res* 49:460–467
51. Champagne FA, Weaver IC, Diorio J, Dymov S, Szyf M, Meaney MJ 2006 Maternal care associated with methylation of the estrogen receptor-alpha1b promoter and estrogen receptor-alpha expression in the medial preoptic area of female offspring. *Endocrinology* 147:2909–2915
52. Lillycrop KA, Slater-Jefferies JL, Hanson MA, Godfrey KM, Jackson AA, Burdge GC 2007 Induction of altered epigenetic regulation of the hepatic glucocorticoid receptor in the offspring of rats fed a protein-restricted diet during pregnancy suggests that reduced DNA methyltransferase-1 expression is involved in impaired DNA methylation and changes in histone modifications. *Br J Nutr* (in press)
53. Han HC, Austin KJ, Nathanielsz PW, Ford SP, Nijland MJ, Hansen TR 2004 Maternal nutrient restriction alters gene expression in the ovine fetal heart. *J Physiol* 558:111–121
54. Oliver MH, Hawkins P, Harding JE 2005 Periconceptional undernutrition alters growth trajectory and metabolic and endocrine responses to fasting in late-gestation fetal sheep. *Pediatr Res* 57:591–598
55. McMillen IC, Robinson JS 2005 Developmental origins of the metabolic syndrome: prediction, plasticity, and programming. *Physiol Rev* 85:571–633
56. Gardner DS, Tingey K, Van Bon BW, Ozanne SE, Wilson V, Dandrea J, Keisler DH, Stephenson T, Symonds ME 2005 Programming of glucose-insulin metabolism in adult sheep after maternal undernutrition. *Am J Physiol Regul Integr Comp Physiol* 289:R947–R954
57. Poore KR, Cleal JK, Newman JP, Boullin JP, Noakes D, Hanson MA, Green LR 2007 Nutritional challenges during development induce sex-specific changes in glucose homeostasis in the adult sheep. *Am J Physiol Endocrinol Metab* 292:E32–E39
58. Torrens C, Brawley L, Anthony FW, Dance CS, Dunn R, Jackson AA, Poston L, Hanson MA 2006 Folate supplementation during pregnancy improves offspring cardiovascular dysfunction induced by protein restriction. *Hypertension* 47:982–987
59. Jackson AA, Dunn RL, Marchand MC, Langley-Evans SC 2002 Increased systolic blood pressure in rats induced by a maternal low-protein diet is reversed by dietary supplementation with glycine. *Clin Sci (Lond)* 103:633–639
60. Brawley L, Torrens C, Anthony FW, Itoh S, Wheeler T, Jackson AA, Clough GF, Poston L, Hanson MA 2004 Glycine rectifies vascular dysfunction induced by dietary protein imbalance during pregnancy. *J Physiol* 554:497–504
61. Drake AJ, Walker BR, Seckl JR 2005 Intergenerational consequences of fetal programming by *in utero* exposure to glucocorticoids in rats. *Am J Physiol Regul Integr Comp Physiol* 288:R34–R38
62. Burdge GC, Slater-Jefferies J, Torrens C, Phillips ES, Hanson MA, Lillycrop KA, 2007 Dietary protein restriction of pregnant rats in the F0 generation induces altered methylation of hepatic gene promoters in the adult male offspring in the F1 and F2 generations. *Br J Nutr* 97:435–439
63. Gluckman PD, Hanson MA, Spencer HG 2005 Predictive adaptive responses and human evolution. *Trends Ecol Evol* 20:527–533
64. Lister AM 2004 The impact of Quaternary Ice Ages on mammalian evolution. *Philos Trans R Soc Lond B Biol Sci* 359:221–241
65. Jablonka E, Oborny B, Molnar I, Kisdí E, Hofbauer J, Czaran T 1995 The adaptive advantage of phenotypic memory in changing environments. *Philos Trans R Soc Lond B Biol Sci* 350:133–141
66. Moran NA 1992 The evolutionary maintenance of alternative phenotypes. *Am Nat* 139:971–989
67. Sultan SE, Spencer HG 2002 Metapopulation structure favors plasticity over local adaptation. *Am Nat* 160:271–283
68. Gluckman PD, Hanson MA 2004 Maternal constraint of fetal growth and its consequences. *Semin Fetal Neonatal Med* 9:419–425
69. Kuzawa CW 1998 Adipose tissue in human infancy and childhood: an evolutionary perspective. *Am J Phys Anthropol* 27:177–209
70. Popkin BM 2001 Nutrition in transition: the changing global nutrition challenge. *Asia Pac J Clin Nutr* 10:S13–S18
71. Bhargava SK, Sachdev HS, Fall CH, Osmond C, Lakshmy R, Barker DJ, Biswas SK, Ramji S, Prabhakaran D, Reddy KS 2004 Relation of serial changes in childhood body-mass index to impaired glucose tolerance in young adulthood. *N Engl J Med* 350:865–875
72. Prentice AM, Moore SE 2005 Early programming of adult diseases in resource poor countries. *Arch Dis Child* 90:429–432
73. Gluckman PD, Hanson MA 2004 The developmental origins of the metabolic syndrome. *Trends Endocrinol Metab* 15:183–187
74. Anway MD, Cupp AS, Uzumcu M, Skinner MK 2005 Epigenetic transgenerational actions of endocrine disruptors and male fertility. *Science* 308:1466–1469
75. Forsen T, Eriksson JG, Tuomilehto J, Teramo K, Osmond C, Barker DJ 1997 Mother's weight in pregnancy and coronary heart disease in a cohort of Finnish men: follow up study. *BMJ* 315:837–840
76. Silverman BL, Purdy LP, Metzger BE 1996 The intrauterine environment: implications for the offspring of diabetic mothers. *Diabetes Rev* 4:21–35
77. Aerts L, Van Assche FA 2006 Animal evidence for the transgenerational development of diabetes mellitus. *Int J Biochem Cell Biol* 38:894–903
78. Fraga MF, Ballestar E, Paz MF, Ropero S, Setien F, Ballestar ML, Heine-Suner D, Cigudosa JC, Urioste M, Benitez J, Boix-Chornet M, Sanchez-Aguilera A, Ling C, Carlsson E, Poulsen P, Vaag A, Stephan Z, Spector TD, Wu YZ, Plass C, Esteller M 2005 Epigenetic differences arise during the lifetime of monozygotic twins. *Proc Natl Acad Sci U S A* 102:10604–10609
79. Silva AJ, White R 1988 Inheritance of allelic blueprints for methylation patterns. *Cell* 54:145–152

# Cold-induced epigenetic programming of the sperm enhances brown adipose tissue activity in the offspring

Wenfei Sun<sup>1,9</sup>, Hua Dong<sup>1,9</sup>, Anton S. Becker<sup>1,2,3</sup>, Dianne H. Dapito<sup>1</sup>, Salvatore Modica<sup>1</sup>, Gerald Grandl<sup>1</sup>, Lennart Opitz<sup>1,4</sup>, Vissarion Efthymiou<sup>1</sup>, Leon G. Straub<sup>1</sup>, Gitalee Sarker<sup>1</sup>, Miroslav Balaz<sup>1</sup>, Lucia Balazova<sup>1</sup>, Alik Perdikari<sup>1</sup>, Elke Kiehlmann<sup>1</sup>, Sara Bacanovic<sup>3</sup>, Caroline Zellweger<sup>3</sup>, Daria Peleg-Raibstein<sup>1</sup>, Pawel Pelczar<sup>5</sup>, Wolf Reik<sup>6,7</sup>, Irene A. Burger<sup>3</sup>, Ferdinand von Meyenn<sup>6,8</sup> and Christian Wolfrum<sup>1\*</sup>

**Recent research has focused on environmental effects that control tissue functionality and systemic metabolism. However, whether such stimuli affect human thermogenesis and body mass index (BMI) has not been explored. Here we show retrospectively that the presence of brown adipose tissue (BAT) and the season of conception are linked to BMI in humans. In mice, we demonstrate that cold exposure (CE) of males, but not females, before mating results in improved systemic metabolism and protection from diet-induced obesity of the male offspring. Integrated analyses of the DNA methylome and RNA sequencing of the sperm from male mice revealed several clusters of co-regulated differentially methylated regions (DMRs) and differentially expressed genes (DEGs), suggesting that the improved metabolic health of the offspring was due to enhanced BAT formation and increased neurogenesis. The conclusions are supported by cell-autonomous studies in the offspring that demonstrate an enhanced capacity to form mature active brown adipocytes, improved neuronal density and more norepinephrine release in BAT in response to cold stimulation. Taken together, our results indicate that in humans and in mice, seasonal or experimental CE induces an epigenetic programming of the sperm such that the offspring harbor hyperactive BAT and an improved adaptation to overnutrition and hypothermia.**

In 2016, 39% of all adults worldwide were classified as being overweight (BMI > 25) and 13% as being clinically obese (BMI > 30)<sup>1</sup>. This imposes a burden on society because obesity-associated comorbidities, which are linked to an increase in adipose tissue mass, are the main contributors to overall mortality and health-care costs. Adipose tissue functions as a dynamic endocrine organ<sup>2</sup>, and, therefore, its 'quality' is considered to be an important factor in the development of obesity-associated comorbidities<sup>3</sup>. Adipose tissue can be divided into the functionally and morphologically distinct white adipose tissue (WAT) and BAT<sup>4</sup>. The main function of BAT is energy dissipation via nonshivering thermogenesis<sup>5</sup>, which is enabled by the presence of uncoupling protein 1 (UCP1) in the inner mitochondrial membrane. Thus, brown adipocytes contribute to the maintenance of body temperature during acute and chronic CE<sup>2,6</sup>.

Besides the classical BAT found in rodents in the interscapular area (iBAT), a second type of thermogenic active fat cell (termed beige or brite adipocytes) has been described, which is induced by CE mainly in inguinal WAT (ingWAT)<sup>7</sup>. Analysis of [<sup>18</sup>F]fluorodeoxyglucose (FDG)-PET and FDG-CT scans (hereafter collectively referred to as FDG-PET/CT scans) have demonstrated the presence of active BAT in adult humans in the supraclavicular, paravertebral and deep neck regions<sup>8–13</sup>, and human BAT can be activated

by mild CE or by administration of a specific  $\beta$ 3-adrenergic receptor (ADRB3) agonist<sup>14,15</sup>. The relevance of BAT for physiology was inferred by the association with various metabolic parameters<sup>15</sup>, and it was demonstrated that people with functional BAT can effectively lose weight by a mild cold-stimulation regime<sup>16</sup>.

In recent years, studies have demonstrated a link between paternal preconception nutrient exposure and the phenotype of the offspring<sup>17,18</sup>. Differences in gene expression patterns arise during development and can be retained through mitosis by epigenetic mechanisms<sup>19</sup>. In the context of thermoregulation, it has been shown that environmentally induced changes in gene expression can affect cellular function and thereby also the predisposition to certain diseases<sup>20</sup>. Additionally, changes in the environment can be transmitted to subsequent generations<sup>18,21,22</sup>. More specifically, there have been indications that the season of birth and adult BMI show some correlation<sup>23</sup>. Here we studied the influence of environmental temperature and its effect on systemic metabolism, as well as the contribution of different thermogenic pathways, using human and mouse studies.

## Results

**Cold exposure before conception and during gestation activates brown and brite adipose tissue.** To identify a possible correlation

<sup>1</sup>Institute of Food, Nutrition and Health, ETH Zurich, Schwerzenbach, Switzerland. <sup>2</sup>Institute of Diagnostic and Interventional Radiology, University Hospital of Zurich, Zurich, Switzerland. <sup>3</sup>Clinic of Nuclear Medicine, University Hospital of Zurich, Zurich, Switzerland. <sup>4</sup>Functional Genomics Center Zurich, ETH Zurich–University of Zurich, Zurich, Switzerland. <sup>5</sup>Center for Transgenic Models, University of Basel, Basel, Switzerland. <sup>6</sup>Epigenetics Program, Babraham Institute, Cambridge, UK. <sup>7</sup>Wellcome Trust Sanger Institute, Hinxton, UK. <sup>8</sup>Department of Medical and Molecular Genetics, King's College London, London, UK. <sup>9</sup>These authors contributed equally: Wenfei Sun and Hua Dong. \*e-mail: christian-wolfrum@ethz.ch



between ambient temperature and BAT abundance, we performed a retrospective study of FDG-PET/CT scans from 2007–2015 that were collected from the University Hospital of Zurich ( $n=8,440$  individuals). Representative PET images from two individuals are shown in Supplementary Fig. 1a. Individuals with active BAT were 3.2% more likely to have been conceived in the colder period of the year, for example, between October and February (mean temperature estimate 2°C), whereas individuals without active BAT were more likely to have been conceived in the warmer months, for example, between April and September (mean temperature estimate 13°C) (Fig. 1a). No apparent fluctuations in age (Supplementary Fig. 1b) or BMI (Supplementary Fig. 1c) were observed, and the pattern persisted for different BAT activation strengths (Supplementary Fig. 1d). Among individuals who were conceived in the colder period ( $n=3,793$ ), BAT-positive individuals ( $n=235$ ) had a significantly lower BMI (mean 20.9 versus 22.8;  $P<0.001$ ) than age- and sex-matched BAT-negative individuals (Fig. 1b). These data identified a correlation between the season of conception and the propensity to form active BAT; however, given the retrospective nature and the large number of potential confounders, causality could not be inferred. Hence, we investigated the effect of CE before and during conception using mouse model systems. We analyzed offspring groups whose parents had not been exposed to cold (23°C) (group 1) or had been exposed to cold (8°C) either before conception (group 2), before conception and during the first week of gestation (group 3) or before conception and during weeks 1 and 2 of gestation (group 4) (Fig. 1c). Notably, we observed that offspring from parents that were exposed to cold before conception showed higher UCP1 expression in both iBAT and ingWAT under regular housing conditions (RT) (Fig. 1d). When we challenged offspring by CE, the effect on UCP1 expression was markedly enhanced (Fig. 1e and Supplementary Fig. 1e). Taken together, our data indicated that CE of parents before conception or during gestation resulted in higher basal and stimulated UCP1 expression in the iBAT and ingWAT of the offspring.

**The effects of preconception cold exposure are mediated through the paternal lineage.** On the basis of these findings, we analyzed whether the observed effect of CE was transmitted through the paternal (P-CE) or maternal (M-CE) lineage by focusing on the preconception exposure model in all subsequent studies. Notably, we observed that the effects of parental CE on UCP1 expression at RT were mediated by the paternal lineage (Fig. 2a) and that the effect was enhanced in the iBAT and ingWAT of male offspring and in the iBAT of female offspring after stimulation by CE (Fig. 2b and Supplementary Fig. 2a). Also, we could show that offspring from P-CE mice (hereafter referred to as P-CE offspring) had higher UCP1 protein levels than those from control (Ctrl) males at 21 d of age at RT and under thermoneutral (TN) conditions (Supplementary Fig. 2b,c). Analysis of gene expression in the iBAT of P-CE offspring demonstrated higher mRNA expression of several markers of brown-fat function in iBAT (Fig. 2c). We did not observe any changes in litter size and in nursing percentages over the postnatal period (Supplementary Fig. 2d,e), suggesting that alterations in maternal behavior were not the cause for the observed phenotype. To exclude paternal behavior as a confounding factor, we performed *in vitro* fertilization (IVF) with sperm derived from P-CE or Ctrl males. We observed an induction of brown fat marker expression (Supplementary Fig. 2f) and UCP1 protein (Fig. 2d and Supplementary Fig. 2g) in the iBAT of both male and female offspring derived from P-CE versus Ctrl sperm, which was paralleled by a difference in body surface temperature (Supplementary Fig. 2h).

Because brown fat is formed at embryonic day 15.5 (E15.5)<sup>24</sup>, we analyzed whether the observed changes were already present before birth. We could show that in iBAT from E18.5 embryos, *Ucp1* mRNA and other brown fat markers were higher in P-CE than

Ctrl offspring (Supplementary Fig. 2i). Notably, these changes did not translate into an altered birth weight nor did we observe differences in postnatal weight gain (Supplementary Fig. 2j). However, iBAT weight in 7-week-old P-CE mice was significantly higher than Ctrl ( $P=0.003$ ; Supplementary Fig. 2k), suggesting that not only expression of UCP1, but also the formation of iBAT, was enhanced in P-CE offspring. Consistent with this, we could show by immunohistochemical analysis of iBAT and ingWAT that the area of UCP1<sup>+</sup> patches, which denote cells with high levels of UCP1 expression, was higher at RT in both iBAT and ingWAT (Fig. 2e,f). After CE, this phenotype was enhanced in both iBAT and ingWAT (Fig. 2g,h). We also observed a lower lipid droplet size in the ingWAT of P-CE offspring, suggesting more active lipid metabolism (Supplementary Fig. 2l). Furthermore, reduced adipocyte size and greater numbers of UCP1<sup>+</sup> cells were observed in P-CE offspring at 21 d of age at RT or at TN (Supplementary Fig. 2m–o). Taken together, our data demonstrated that the effect of CE was mediated through the paternal lineage and affected both UCP1 expression and adipose tissue morphology.

**Cold exposure of paternal mice induces iBAT activity and systemic metabolism in the offspring.** On the basis of these findings, we analyzed whether the effect of P-CE would translate into a higher thermogenic activity. Surface temperature was higher in P-CE offspring than in Ctrl offspring at postnatal day (P) 7 (Fig. 3a) at RT. At 7 weeks of age, mice had the same body weight (Supplementary Fig. 3a) and the same surface temperature (Fig. 3b) at RT, whereas after CE, the P-CE offspring exhibited a higher surface temperature (Fig. 3b). Furthermore, we observed that P-CE offspring had an 11% higher volume of oxygen consumption rate ( $VO_2$ ) and volume of carbon dioxide production rate ( $VCO_2$ ) at RT, which was enhanced after acute CE (Fig. 3c and Supplementary Fig. 3b), whereas the respiratory exchange ratio (RER) remained unchanged (Supplementary Fig. 3c). Because CE can lead to shivering, we quantified the induction of brown fat in response to an intraperitoneal (i.p.) injection of ADRB3 agonist CL316,243 (CL). We observed higher amounts of UCP1 protein (Fig. 3d) and higher  $VO_2$  and  $VCO_2$  levels (Fig. 3e and Supplementary Fig. 3d), which was concomitant with more UCP1<sup>+</sup> cells in the iBAT (Fig. 3f) of P-CE mice. Of note, we could show a lower RER in P-CE offspring following CL injection, suggesting a preferred utilization of fatty acids (Supplementary Fig. 3e).

On the basis of these data, we analyzed whether the changes in respiration could lead to altered systemic metabolism. We did not observe any changes in body weight between 7 and 18 weeks of age (Supplementary Fig. 3f) when P-CE and Ctrl offspring were fed a regular chow diet at RT. Similarly, we did not observe any change in food intake (Supplementary Fig. 3g); however, we could show that P-CE offspring showed a substantial reduction in basal glucose levels, as well as a trend for improved insulin sensitivity (Supplementary Fig. 3h). Insulin, cholesterol and fibroblast growth factor 21 (FGF21) levels were the same in both groups of offspring (Supplementary Fig. 3i–k), and P-CE offspring showed lower circulating triacylglycerol (TAG) levels (Supplementary Fig. 3l) and higher circulating non-esterified fatty acid (NEFA) levels under fasted conditions (Fig. 3g). To assess whether the changes in altered glucose homeostasis could be due to a higher glucose uptake into iBAT, we injected Ctrl and P-CE offspring at RT or after CE with radiolabeled 2-deoxyglucose. We observed higher glucose uptake exclusively into iBAT and ingWAT of P-CE offspring, whereas glucose uptake in muscle, brain, liver and heart was not affected (Fig. 3h and Supplementary Fig. 3m). These changes were paralleled by an induction of facilitated glucose transporter member 4 (GLUT4) expression in iBAT under CE (Fig. 3i). Taken together, our data demonstrate that P-CE induces brown and brite adipocyte function in the offspring, which leads to an improved systemic metabolism.

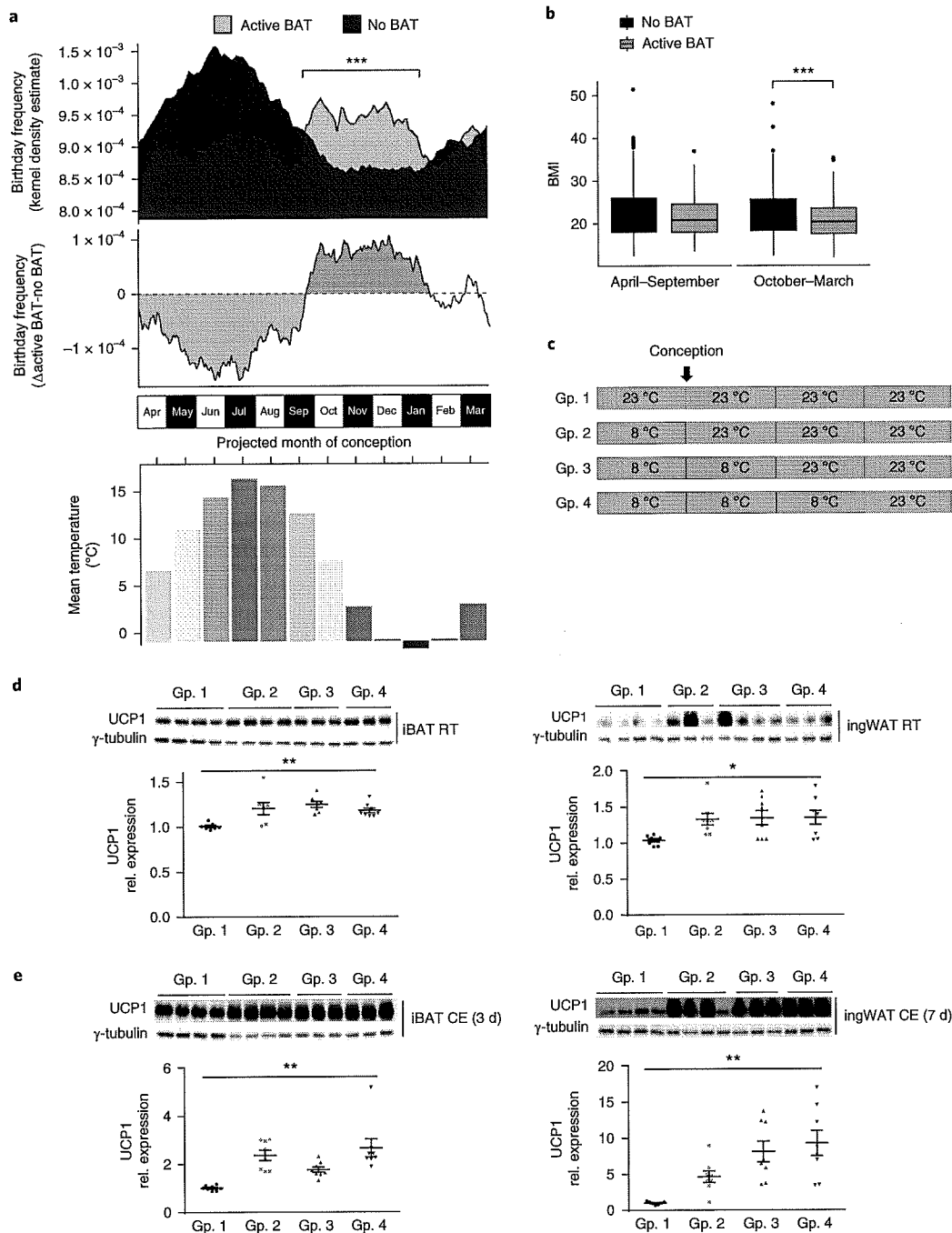


**Fig. 1 | Parental cold exposure induces UCP1 expression in iBAT and ingWAT.** **a**, The birth day frequency of individuals with no active BAT (no BAT) and active BAT (top) and the ratio of such individuals as a function of birth date (middle). BAT activity was measured by FDG-PET/CT scans ( $n=8,440$  individuals,  $P=1 \times 10^{-16}$ ). Bottom, monthly mean temperatures in Switzerland, to serve as a visual illustration of the warmer and colder periods. **b**, BMI of BAT-negative (black boxes) and BAT-positive (green boxes) individuals born between April and September and between October and March ( $n=914$  individuals). Vertical bars are estimated 95% confidence intervals (CIs); the middle line represents the median, the top and bottom line the 75th and 25th percentile, respectively, the whiskers have the length of  $1.5 \times$  the interquartile range.  $P=0.00091$  by two-sided  $t$ -test, Bonferroni-corrected. **c**, Scheme for the parental CE mouse model. 10-week-old male and female C57BL/6 mice were cold-stimulated for 0 (group 1; Gp. 1), 7 (group 2; Gp. 2), 14 (group 3; Gp. 3) or 21 d (group 4; Gp. 4) at  $8^{\circ}\text{C}$ , then returned to  $23^{\circ}\text{C}$ . Each block denotes 1 week; breeding was initiated at the end of the block 1. **d,e**, Cropped western blots of UCP1 ( $\gamma$ -tubulin is the loading control) in iBAT and ingWAT from the four experimental groups of offspring described in **c**; tissues were isolated while the mice were at RT (**d**) or after CE (**e**). Shown is one representative blot from four independent experiments; graphs depict mean of litter from all experiments  $\pm$  s.e.m.;  $n$ =number of litters tested, each dot represents one litter. Results are mean  $\pm$  s.e.m. (**d**, left:  $n=7$ ,  $F_{(3,24)}=6.48$ ; **d**, right:  $n=8$ ,  $F_{(3,28)}=3.52$ ; **e**, left:  $n=8$ ,  $F_{(3,28)}=10.90$ ; **e**, right:  $n=8$ ,  $F_{(3,28)}=8.65$ ). Statistical significance was calculated using one-way analysis of variance (ANOVA); \* $P < 0.05$ , \*\* $P < 0.01$ , \*\*\* $P < 0.001$ .

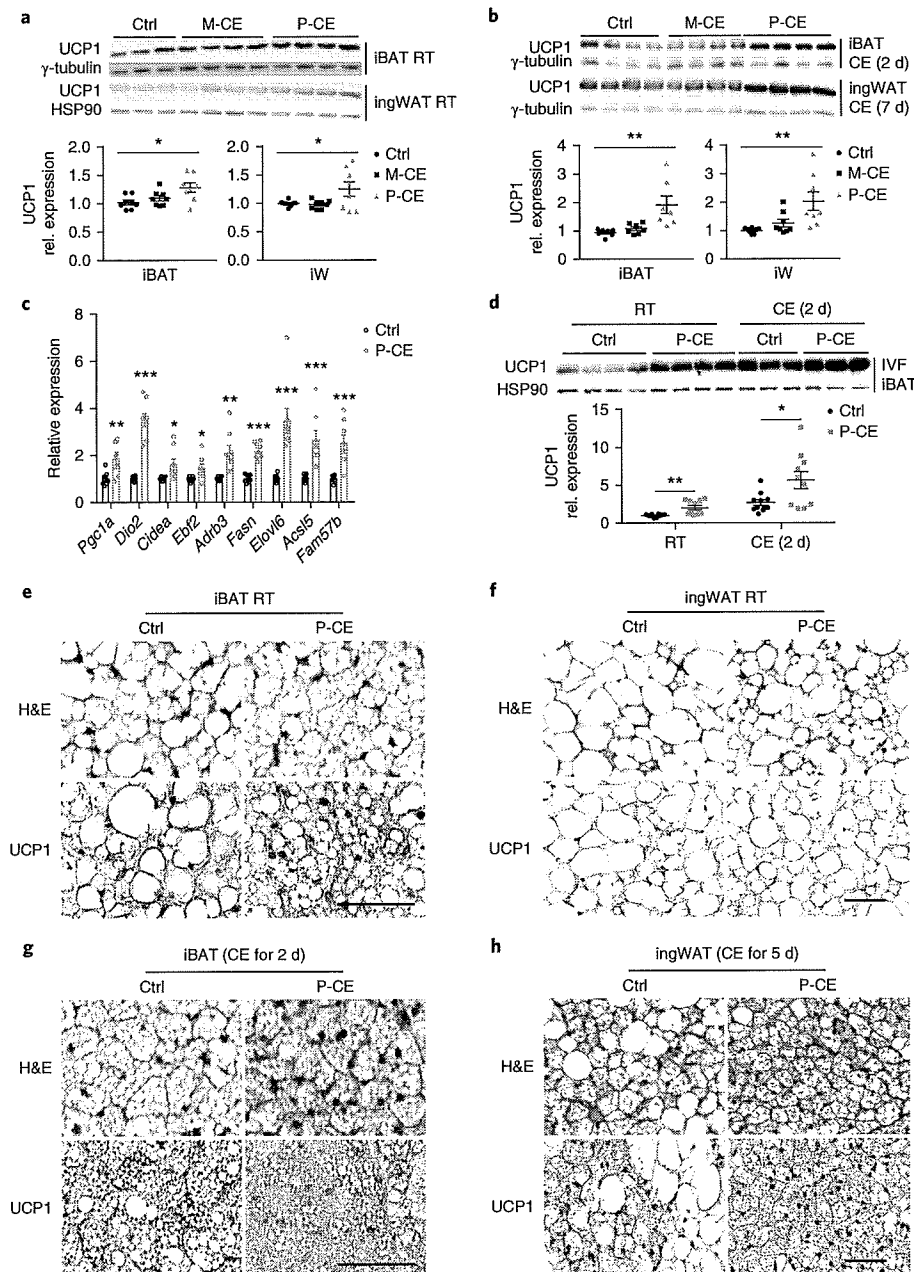


**Fig. 2 | Paternal cold exposure exclusively induces UCP1 expression in iBAT and ingWAT.** **a,b**, Either female (M-CE) or male (P-CE) mice were cold-stimulated for 7 d before initiating a mating. All mice were kept at 23°C afterwards. Shown are cropped western blots of UCP1 ( $\gamma$ -tubulin and HSP90 were used as loading controls) from iBAT and ingWAT isolated from mice in the three experimental groups of offspring of Ctrl, M-CE and P-CE while the mice were at RT (**a**) or after CE (**b**). **c**, mRNA levels of different brown fat markers in the iBAT of Ctrl and P-CE offspring at RT ( $n=8$  litters per group). Expression was normalized by  $\Delta C_t$  values. **d**, Cropped western blots of UCP1 in the iBAT (HSP90 was used as the loading control) from the IVF offspring of Ctrl and P-CE at RT and after 2 d of CE, ( $n=11$  litters for Ctrl;  $n=10$  litters for P-CE). **e–h**, Representative hematoxylin and eosin (H&E) and UCP1 immunohistochemistry staining of iBAT (**e,g**) and ingWAT (**f,h**) from Ctrl or P-CE offspring at 23°C (**e,f**) and 8°C (**g,h**). **e,f**:  $n=8$  litters per group, **g,h**:  $n=6$  litters per group. Scale bar, 100  $\mu$ m. Throughout, data are mean  $\pm$  s.e.m.; each dot represents one litter ( $n$ =litters per group; **a**, left:  $n=8$ ,  $F_{(2,21)}=4.93$ ,  $P=0.018$ ; **a**, right:  $n=8$ ,  $F_{(2,21)}=3.92$ ,  $P=0.036$ ; **b**, left:  $n=7$ ,  $F_{(2,18)}=8.27$ ,  $P=0.003$ ; **b**, right:  $n=8$ ,  $F_{(2,21)}=7.74$ ,  $P=0.003$ ; **d**, left:  $P=0.003$ ; **d**, right:  $P=0.02$ ). \* $P<0.05$ ; \*\* $P<0.01$ ; \*\*\* $P<0.001$ ; by one-way ANOVA (**a,b**) or two-tailed unpaired Student's  $t$ -test (**c,d**).

**The effect of cold-exposed paternal mice is mediated in part through brown and brite adipocytes.** Because several tissues contribute to the maintenance of body temperature, we next aimed to assess the contribution of brown and brite adipocytes. Therefore,

we used a transgenic mouse line that expressed a diphtheria toxin receptor (DTR) fused to green fluorescent protein (GFP) under the control of the *Ucp1* promoter (hereafter referred to as *Ucp1*-DTR-GFP mice)<sup>25</sup>. Sequential injections of diphtheria toxin A (DTA)

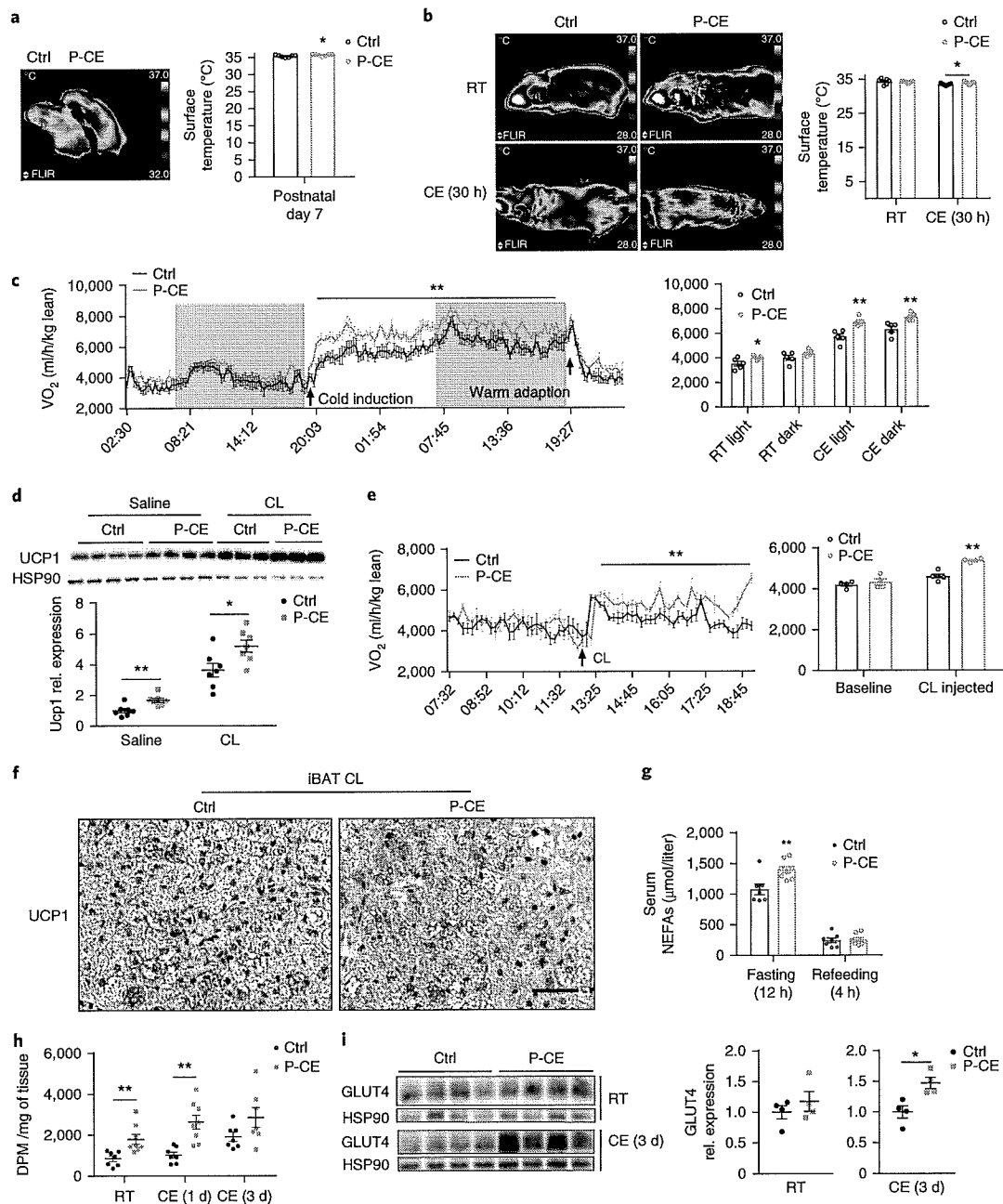


**Fig. 3 | Paternal cold exposure induces oxygen consumption in offspring after cold or ADRB3 agonist stimulation.** **a**, Left, representative thermographic image of Ctrl and P-CE offspring at postnatal day 7. Offspring were kept at RT. Right, calculated averages of surface temperature ( $n = 7$  litters).  $P = 0.04$ . **b**, Representative thermographic image (left) and calculated averages of surface temperature (right) of Ctrl and P-CE offspring at 23 °C and after 30 h of CE ( $n = 7$  litters).  $P$  (30-h CE) = 0.03. **c**, Time-resolved oxygen consumption in Ctrl and P-CE offspring mice, with cold induction (arrow) followed by warm adaption (arrow); dark phase is marked as dark background; right inset depicts calculated means as indicated ( $n = 5$  litters).  $P = 0.006$ . **d**, Cropped western blots of UCP1 from iBAT (HSP90 was used as the loading control) of Ctrl and P-CE offspring that were injected with saline or CL (0.1 mg per kg body weight, three times, every 24 h,  $n = 7$  litters). **e**, Time-resolved oxygen consumption of Ctrl ( $n = 4$  litters) and P-CE ( $n = 5$  litters) offspring, before and after (arrow) injection of CL (arrow).  $P = 0.003$ . **f**, Representative images of UCP1 staining of iBAT from Ctrl or P-CE offspring after injection with CL ( $n = 6$  litters per group). Scale bar, 100  $\mu\text{m}$ . **g**, Serum NEFAs level of fasted (12 h) and re-fed (4 h) mice from the Ctrl ( $n = 7$  litters) and P-CE ( $n = 8$  litters) groups. **h**, Glucose uptake in BAT at RT, after 1 d or 3 d of CE ( $n = 7$  litters for all groups, except  $n = 8$  for the P-CE at RT and 1 d CE groups). **i**, Western blots of GLUT4 in the iBAT (HSP90 was used as the loading control) isolated from Ctrl or P-CE offspring at RT and after 3 d of CE ( $n = 4$  litters). Throughout, results are mean  $\pm$  s.e.m.; each dot represents one litter. Statistical significance was calculated by a two-tailed unpaired Student's *t*-test; \* $P < 0.05$ , \*\* $P < 0.01$ .



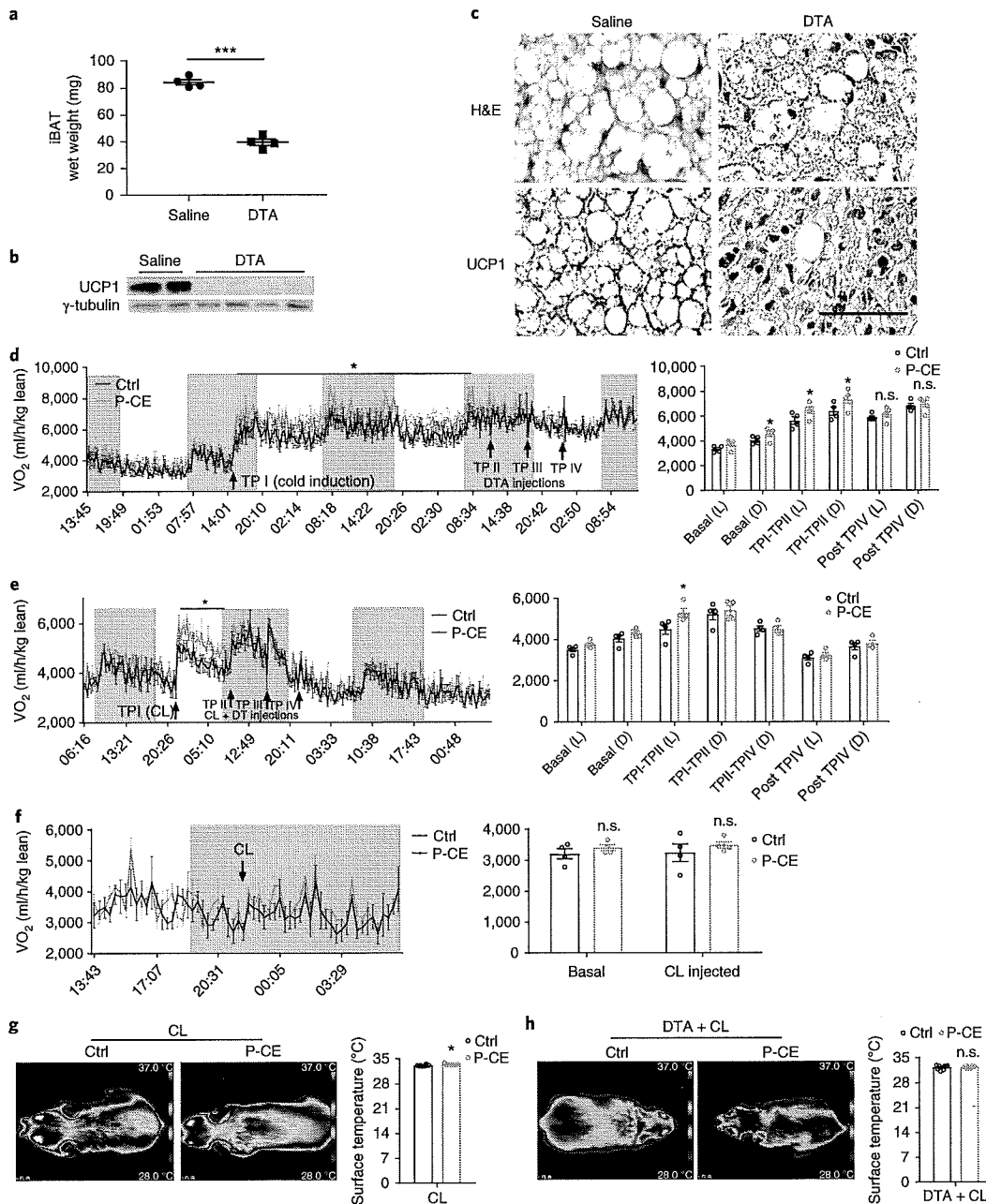


**Fig. 4 | Paternal cold exposure induces oxygen consumption in offspring due to increased BAT functionality. a,b**, Tissue wet weight ( $n = 4$  mice per group;  $P = 0.000001$ ) (**a**) and cropped western blots of UCP1 in the iBAT ( $\gamma$ -tubulin was used as the loading control) (**b**) from *Ucp1-DTR-GFP* mice (11-weeks of age) after treatment with saline or DTA. **c**, Representative H&E (top) and UCP1 (bottom) staining of iBAT from *Ucp1-DTR-GFP* mice after saline (left) or DTA (right) injection ( $n = 4$  mice per group). Scale bar, 100  $\mu\text{m}$ . **d**, Time-resolved oxygen consumption in *Ucp1-DTR-GFP* Ctrl ( $n = 4$  litters) and P-CE ( $n = 5$  litters) offspring after cold induction (TP I) followed by three DTA injections (TP II–IV). Graph shows calculated means as indicated in the light cycle (L) and dark cycle (D); dark phase is marked as dark background.  $P = 0.04$ . **e**, Time-resolved oxygen consumption in *Ucp1-DTR-GFP* Ctrl and P-CE offspring after CL injection (TP I) followed by three DTA + CL injections (TP II–IV). Graph depicts calculated mean as indicated ( $n = 4$  litters).  $P = 0.03$ . **f**, Time-resolved oxygen consumption in *Ucp1-DTR-GFP* Ctrl and P-CE offspring 24 h after BAT depletion (TP IV in **e**) and stimulation with CL (arrow) ( $n = 4$  litters). **g,h**, Representative thermographic images of Ctrl and P-CE offspring that were subjected to CL stimulation before (**g**) or after (**h**) BAT depletion. Graphs depict calculated averages ( $n = 8$  litters). Throughout, results are mean  $\pm$  s.e.m. Statistical significance was calculated by a two-tailed unpaired Student's *t*-test; \* $P < 0.05$ , \*\*\* $P < 0.001$ ; n.s., not significant.

in these mice led to the complete ablation of brown adipocytes, as indicated by the reduction in iBAT mass (Fig. 4a) and loss of UCP1 protein expression in the iBAT (Fig. 4b,c). Similar to wild-type P-CE

offspring, P-CE offspring from the *Ucp1-DTR-GFP* line exhibited slightly higher  $\text{VO}_2$  and  $\text{VCO}_2$  at RT and a significant induction of both parameters after CE at time point I (TP I) (Fig. 4d

and Supplementary Fig. 4a, TP I). When mice were treated with DTA (TP II–IV), we observed a reduction in  $VO_2$  and  $VCO_2$  exclusively in the P-CE offspring (Fig. 4d and Supplementary Fig. 4a, TP II–IV), which, after three consecutive injections of DTA, led to the abrogation of the difference in  $VO_2$  and  $VCO_2$  levels. The RER was not altered between the two groups at any time point (Supplementary Fig. 4b).

To avoid a shivering response in mice that received DTA injections, we analyzed respiration in mice in response to CL injections. We observed higher  $VO_2$  and  $VCO_2$  in P-CE versus Ctrl offspring of *Ucp1*-DTR-GFP mice after CL treatment (Fig. 4e and Supplementary Fig. 4c, TP I). Because the CL injections caused only a transient increase in respiration, we treated the mice with three subsequent injections of CL and DTA (Fig. 4e and Supplementary Fig. 4c, TP II–IV). After two injections with DTA the difference between P-CE and Ctrl offspring on both  $VO_2$  and  $VCO_2$  was lost, suggesting that brown and brite adipocytes might, in part, be responsible for the observed higher respiration in P-CE offspring. Similarly, we observed a lower RER in P-CE offspring after CL injections, which was lost after DTA injections (Supplementary Fig. 4d). These findings were supported by the observation that 24h after the third CL + DTA injection, we did not observe any difference in respiration between both groups (Fig. 4f and Supplementary Fig. 4e,f). To analyze whether the observed effects would also translate into an induction of thermogenesis, we quantified surface temperature after an injection of CL, with or without DTA-mediated ablation of brown adipocytes. In accordance with previous data (Fig. 4e), surface temperature was higher in P-CE versus Ctrl offspring after the CL injection (Fig. 4g), and the effect was lost when brown adipocytes were ablated (Fig. 4h). Lastly, we could show that DTA injection did not induce overt inflammation in mice (Supplementary Fig. 4g). Taken together, our data demonstrated that the effect of P-CE on respiration and thermogenesis was, at least in part, mediated through the activation of brown adipocytes.

**Cold exposure of paternal mice protects from diet-induced obesity and insulin resistance.** Because BAT has been implicated in energy expenditure, we aimed to assess whether body weight and metabolism would be different under challenged conditions. Therefore, we fed P-CE and Ctrl offspring a high-fat diet (HFD), in which 60% of the calories were derived from fat, for 10 weeks. Even though P-CE offspring consumed significantly more food than Ctrl offspring (Fig. 5a), we found that P-CE offspring showed slightly lower body weight gain and reduced fat mass than Ctrl offspring (Fig. 5b,c). Furthermore, we found that P-CE offspring had markedly better insulin sensitivity than Ctrl offspring (Fig. 5d), even though fasting blood glucose levels were similar in both groups of mice. The latter might be due to the lower levels of circulating insulin in P-CE offspring (Fig. 5e). We found significantly lower levels of circulating TAGs in P-CE versus Ctrl offspring (Fig. 5f), whereas there was no difference in cholesterol levels (Fig. 5g).

Of note, we observed a significantly higher metabolic rate indicated by higher  $VO_2$  and  $VCO_2$  levels at RT conditions in P-CE versus Ctrl offspring (Fig. 5h and Supplementary Fig. 5a), whereas we did not observe any changes in substrate utilization, as indicated by an unchanged RER (Supplementary Fig. 5b). This higher oxygen consumption rate (OCR) was paralleled by significantly higher body surface temperature (Supplementary Fig. 5c) and *UCP1* expression in iBAT (Supplementary Fig. 5d). Furthermore, we could show that hepatic lipid accumulation was reduced in P-CE versus Ctrl offspring (Fig. 5i,j), which might explain the altered insulin sensitivity. Notably, circulating levels of FGF21, a hormone which has been suggested to be secreted from activated BAT<sup>26</sup> and is known to affect glucose and lipid homeostasis, was higher in P-CE offspring kept on a HFD (Fig. 5k). Taken together, our data demonstrate that under RT conditions, which give mild cold stress, P-CE offspring

are partially protected from diet induced obesity and maintain an improved metabolic profile.

**Gene expression and DNA methylation analysis of P-CE offspring suggests changes in brown adipocyte formation and neurogenesis.** We then asked whether transcriptional changes in iBAT could explain the observed phenotype. Therefore, we performed RNA sequencing (RNA-seq) analysis of iBAT from P-CE and Ctrl offspring at RT and after CE for 3 d. Unbiased hierarchical clustering, including that for all of the genes expressed in at least one sample group, revealed distinct transcriptional profiles for the different conditions (Supplementary Fig. 6a). A principal component analysis (PCA) similarly showed distinct clusters of each of the four sample groups (Fig. 6a). Principal component 1 (PC1) seemed to capture the differences imposed by acute CE. Several genes related to BAT activity, such as glycerol kinase (*Gyk*) or *Ucp1*, were major contributors of negative PC1 loadings, whereas muscle-specific genes contributed to positive PC1 loadings. Notably, samples from P-CE offspring after CE had an even stronger negative PC1 loading than the Ctrl samples, indicating a hyperactivated BAT condition in P-CE offspring.

A pairwise differential gene expression analysis that compared Ctrl offspring at RT versus after CE (Ctrl-RT versus Ctrl-CE) and that considered at least a twofold mean expression difference to be significant (Supplementary Table 1) identified many genes related to BAT activity (Supplementary Fig. 6b,c). Consistent with the PCA, we also found a number of genes that were upregulated in the CE samples from P-CE offspring versus Ctrl offspring to be related to BAT activity (Fig. 6b), as well as an enrichment of gene ontology (GO) terms related to high metabolic activity in all significantly regulated genes (Fig. 6c). Of note, *Adrb3* and *Ucp1* were also significantly differentially expressed; however, the regulation was <2-fold between cold-exposed P-CE and Ctrl offspring; therefore, these genes were not included in the GO analysis.

Because phenotypic and transcriptional changes of P-CE offspring are mediated through the sperm via the paternal lineage, we performed whole-genome bisulphite sequencing (WGBS) of sperm (sixfold average genomic coverage in each sample) to identify possible DNA methylation alterations that could potentially mediate the intergenerational transmission of the observed phenotype (Fig. 6d). We observed a small but significantly greater degree of global 5'-cytosine-phosphate-guanine-3' (CpG) DNA methylation in the P-CE samples (89.5% versus 87.5%; *P* value < 0.002; Fig. 6e), which indicated an effect of CE on the sperm methylome.

To analyze whether methylation levels were altered in genomic regions that might affect gene expression in the offspring, we first performed hierarchical clustering and PCA of the methylation status of all promoter regions (Fig. 6f and Supplementary Fig. 6d). We observed a clear separation between P-CE and Ctrl sperm samples and a distinguishable clustering of the two groups in the PCA. In contrast to global CpG methylation, we found a small, but significant, reduction in the average methylation levels of CpG islands (CGI) in the P-CE samples (Supplementary Fig. 6e). Hierarchical clustering and PCA of all non-CGI promoters showed comparable levels of separation on PC1 but less clear clustering, suggesting that the differences in CGI methylation were relevant contributors to the observed differences in promoter methylation.

These analyses indicated that the CE-induced methylation changes in sperm were reproducible and contributed to the observed phenotypic differences in the offspring. It is important to note that sperm is a haploid cell type, and as such, single CpG sites can only be either methylated or unmethylated. To address this issue, we decided to subdivide the genome in probes of 50 adjacent CpGs and analyze methylation changes over these probes. An unbiased analysis of the P-CE and Ctrl sperm methylome datasets identified 2,431 DMRs with an overlapping or downstream (maximum 2 kb)

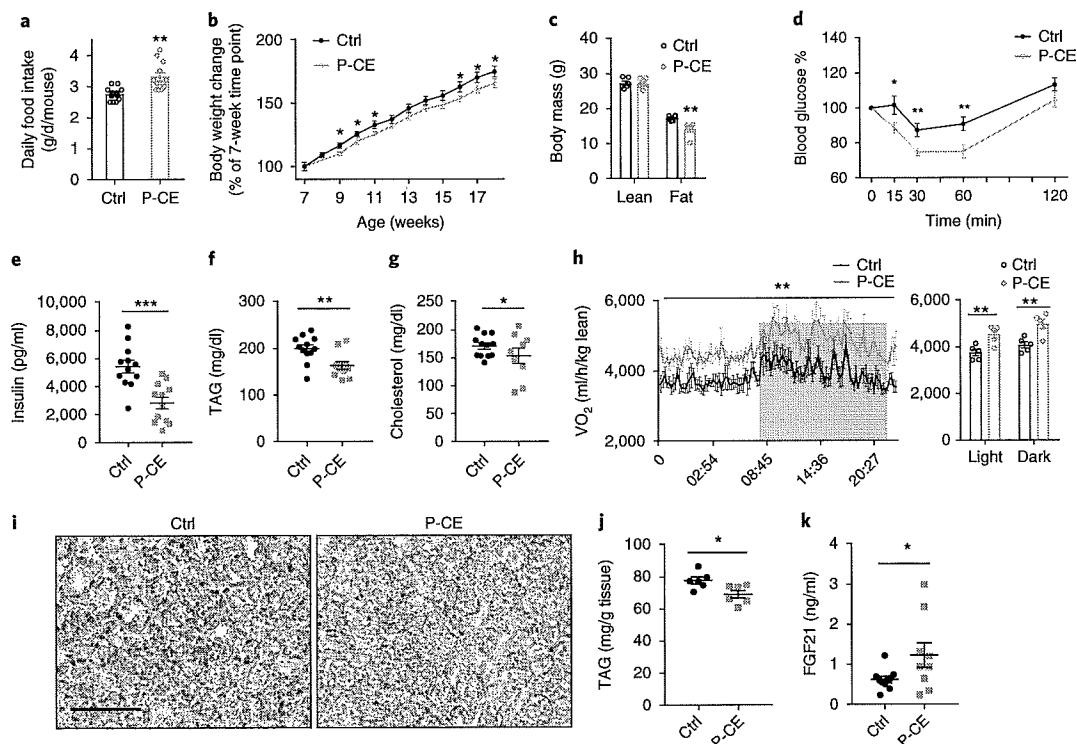


**Fig. 5 | Paternal cold exposure protects offspring from high-fat-diet-induced obesity. a–c**, Daily food intake ( $n=12$ ) (**a**), body weight gain ( $n=11$ ) (**b**) and body composition ( $n=6$ ) (**c**) of Ctrl and P-CE offspring mice that were fed a HFD, at RT for the indicated amounts of time. **d**, Insulin tolerance test of Ctrl or P-CE offspring that were fed a HFD for 7 weeks at RT, with 6 h of fasting ( $n=12$ ). Shown is one representative of three independent experiments. **e–g**, Circulating insulin ( $n=12$ ) (**e**), TAG ( $n=11$ ) (**f**) and cholesterol ( $n=9$ ) (**g**) levels of Ctrl or P-CE offspring that were fed a HFD for 11 weeks at RT. **h**, Time-resolved oxygen consumption time course and analysis of Ctrl or P-CE offspring that were fed a HFD for 11 weeks at RT. Graph depicts calculated mean as indicated ( $n=5$ ).  $P=0.001$ . **i**, Representative Oil red O staining on liver sections of Ctrl or P-CE offspring that were fed a HFD for 11 weeks at RT ( $n=6$  litters). Scale bar, 200  $\mu\text{m}$ . **j**, TAG content in the liver of the indicated mice ( $n=6$ ). **k**, Circulating FGF21 levels of Ctrl or P-CE offspring on a HFD ( $n=9$ ). Throughout, results are mean  $\pm$  s.e.m.;  $n$ =number of litters tested, each dot represents one litter. Statistical significance was calculated by a two-tailed unpaired Student's  $t$ -test; \* $P<0.05$ , \*\* $P<0.01$ , \*\*\* $P<0.001$ .

gene (Fig. 6g and Supplementary Table 2). GO enrichment analysis of DMRs that were hypomethylated in the P-CE samples showed a relation to many 'neurogenesis' terms (Fig. 6g). A specific analysis of *Adrb3*, which encodes an important regulator of BAT activity, revealed local hypomethylation in the coding region (false discovery rate (FDR)=0.01). An independent pyrosequencing analysis of individual CpG sites at the *Adrb3* locus in sperm samples confirmed this result (Supplementary Fig. 6f) and showed that the CpGs at the *Adrb3* locus were hypomethylated in the iBAT and ingWAT from adult P-CE mice (Supplementary Fig. 6g,h). Notably, the transcriptomic analysis had shown that *Adrb3* was also significantly more highly expressed in P-CE iBAT than Ctrl iBAT (Figs. 2c and 6b). To test whether this effect was mediated by DNA methylation, we generated an *Adrb3* overexpression plasmid with a CpG-free backbone and in which all (or none, as control) of the CpGs of *Adrb3* had been methylated *in vitro*. We then transfected the methylated and nonmethylated plasmids into cells that did not express *Adrb3* (Supplementary Fig. 6i) and confirmed the methylation status of the CpG sites in the transfected plasmids (Supplementary Fig. 6j). We found that expression of *Adrb3* from the methylated plasmid was significantly lower than that from the unmethylated plasmid, suggesting that DNA methylation at the *Adrb3* locus influenced *Adrb3* expression.

Next we elucidated whether the differential methylation status in the sperm of the P-CE and Ctrl samples was directly correlated with transcriptional changes in iBAT tissue. Therefore, we analyzed the

expression levels of genes that overlapped with DMRs and that were either hypermethylated or hypomethylated in P-CE sperm. Of note, we found that the average expression levels of transcripts that overlapped with hypermethylated sperm P-CE DMRs were significantly increased as compared to the expression levels for all transcripts, whereas inversely, the expression of transcripts that overlapped with hypomethylated DMRs was significantly lower than the expression of all transcripts in iBAT tissue (Fig. 6h). Gene body methylation is a feature of transcribed genes, although the exact functions are not known<sup>27,28</sup>, and it is therefore possible that the identified sperm DMRs could contribute to the greater formation of iBAT tissue in P-CE animals and might contribute to the observed intergenerational effect. We also found that a number of transcripts were significantly differentially expressed in the iBAT of cold-exposed P-CE versus Ctrl samples and that they overlapped with hypo- or hypermethylated DMRs in the respective sperm samples, highlighting a potential direct effect of germline methylation levels and iBAT expression levels for selected genes (Fig. 6i). Taken together, our analyses support our findings that the iBAT from P-CE mice is hyperactivated, which is, in part, dependent on enhanced brown adipocyte formation, as reflected by the upregulated brown adipocyte markers and downregulated muscle-specific genes, possibly due to increased neuronal innervation.

**P-CE leads to a cell autonomous increase in brown adipocyte formation.** To assess whether brown adipocyte formation was

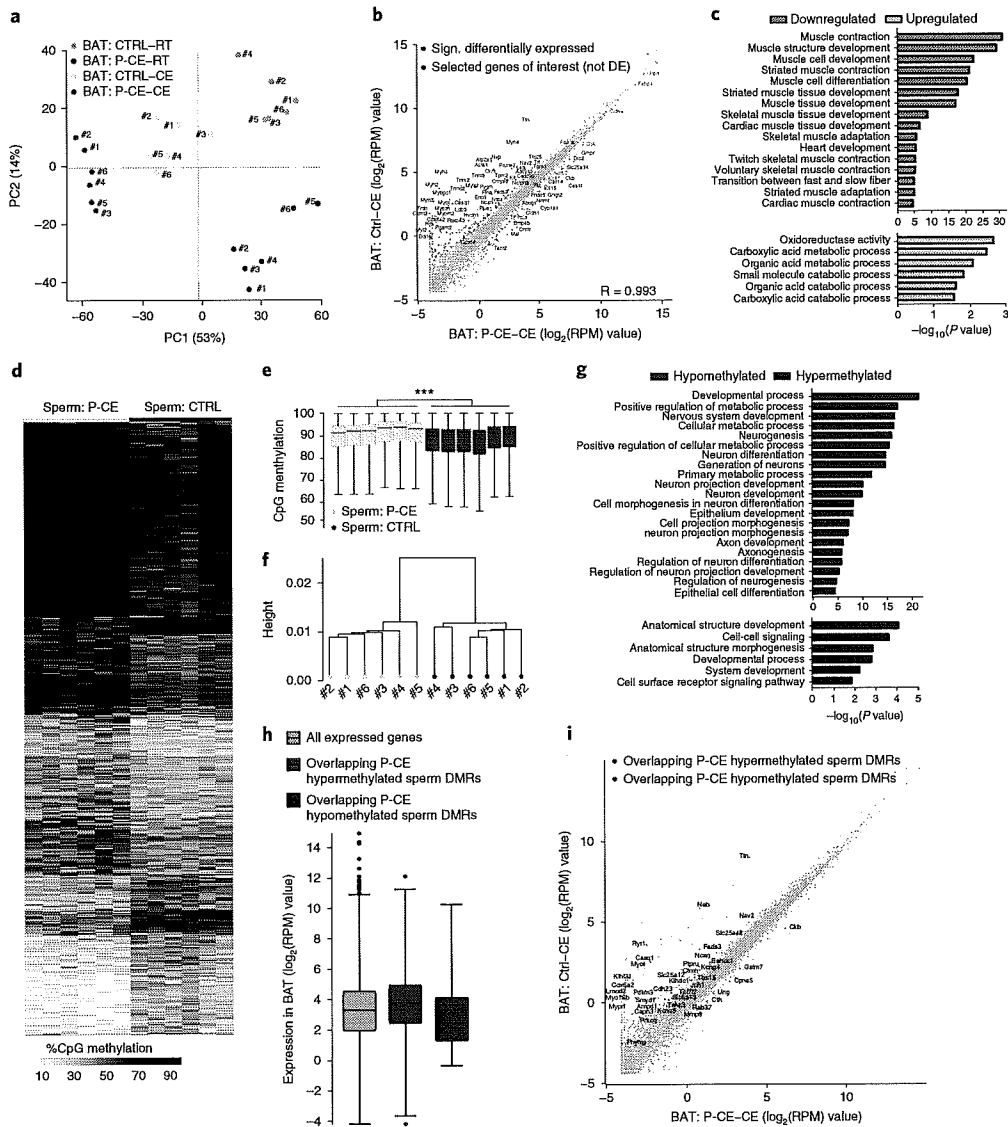


**Fig. 6 | Paternal cold exposure affects the transcriptional signature of the brown adipose tissue in the offspring and the epigenetic profile of the sperm.** **a**, PCA of RNA-seq data from BAT samples. PC1 and PC2 for each sample were calculated using the SeqMonk PCA pipeline ( $n = 6$  litters). **b**, Scatter plot of RNA-seq data from BAT samples, comparing P-CE versus Ctrl samples following 3 d of CE. Plotted are the  $\log_2$ -transformed normalized reads per million (RPM) values. Significant DEGs (overlap between DEseq2 and EdgeR) with at least twofold mean expression differences are highlighted in red. Selected genes of interest that did not fulfill all of the above criteria are labeled in blue and are only shown for comparison with the literature, ( $n = 6$ ). **c**, GO terms of upregulated and downregulated genes in iBAT samples from cold-exposed P-CE versus Ctrl offspring ( $n = 6$  litters). **d**, Heat map showing the methylation levels in DMRs between P-CE and Ctrl sperm samples ( $n = 6$  mice per group). Clustering of DMRs was performed in SeqMonk. **e**, Box-and-whisker plots showing the CpG methylation levels of individual replicates of sperm samples from P-CE and Ctrl samples. Methylation was quantified over consecutive probes spanning 50 CpGs. Significance was calculated by using the mean CpG methylation levels of P-CE versus Ctrl samples by a two-tailed unpaired Student's  $t$ -test ( $n = 6$  mice).  $P = 0.00052$ . **f**, Hierarchical clustering of promoter CpG methylation levels. **g**, GO terms of hyper- and hypo-DMRs in P-CE versus RT sperm ( $n = 6$  mice). **h**, Expression levels of transcripts in BAT samples that overlap with sperm DMRs that are either hypermethylated or hypomethylated in the paternal CE versus control samples. Shown are the  $\log_2(\text{RPM})$  values of gene expression levels in BAT ( $n = 6$  mice). Significance was calculated from the average gene expression levels of each group by a two-tailed unpaired Student's  $t$ -test. Number of all expressed genes is 11,334; number of genes that overlapped with P-CE hypermethylated sperm DMRs is 1,049; number of genes that overlapped with P-CE hypomethylated sperm DMRs is 365; "All expressed genes" versus "Genes overlapping P-CE Hypermethylated Sperm DMRs",  $P = 3.7 \times 10^{-14}$ ; "All expressed genes" versus "Genes overlapping P-CE Hypomethylated Sperm DMRs",  $P = 1.4 \times 10^{-6}$ . Any individual points that fall outside this range are shown as filled circles. Each circle represents a single probe. **i**, Scatter plot of RNA-seq data from BAT samples, comparing P-CE versus Ctrl samples following 3 d of CE. Plotted are the  $\log_2$ -transformed normalized RPM values. Highlighted are all genes that were significantly differentially expressed (overlap between DEseq2 and EdgeR with at least twofold mean expression differences) in samples between 3-d cold-exposed P-CE and Ctrl mice and that overlapped with identified sperm DMRs. In **e, h**, shown are box plots of the CpG methylation percentages of tiling probes spanning 50 CpGs each; the middle line indicates the median of the data; the upper and lower extremities of the box show the 25th and 75th percentiles; and the upper and lower black whiskers show the median  $\pm$  the interquartile range (25–75%) multiplied by 2. \*\*\* $P < 0.001$ .



indeed altered in P-CE offspring, we isolated the stromal vascular fraction (SVF) from the iBAT of P-CE and Ctrl mice and differentiated these cells into mature brown adipocytes *ex vivo*. When we analyzed lipid droplet staining, we did not observe any differences between the two groups of cells in either cell numbers or the appearance of multilocular cells (Supplementary Fig. 7a–c). However, we observed a significant increase in the percentage of UCP1<sup>+</sup> cells but not in the average intensity of UCP1 staining in UCP1<sup>+</sup> cells (Supplementary Fig. 7a,d,e), suggesting that there was an increased propensity to form brown adipocytes. We observed a significant induction of UCP1 protein and *Ucp1* mRNA in P-CE-offspring-derived cells (Supplementary Fig. 7f,g). Similar to our observations for UCP1, we observed a higher mRNA expression of *Adrb3* and cell-death-inducing DFFA-like effector A (*Cidea*) in P-CE-offspring-derived cells, whereas peroxisome proliferator-activated receptor gamma (*Pparg*) levels were the same (Supplementary Fig. 7h–j).

To analyze whether these changes would translate into altered functionality, we quantified the OCR of these *ex vivo*-differentiated cells. Although we did not observe any changes in basal OCR, we could show that cells from P-CE offspring had a significantly higher OCR than cells from Ctrl offspring under CL-stimulated conditions (Supplementary Fig. 7k).

To confirm these findings, we quantified ADRB3 protein levels in P-CE and Ctrl offspring. In accordance with the mRNA data, we observed higher ADRB3 expression in P-CE offspring than in Ctrl offspring at the RT, CE and TN conditions (Supplementary Fig. 7l). Given the widespread expression of *Adrb3*, we also analyzed its expression in ingWAT, epididymal adipose tissue (epiWAT) and heart (Supplementary Fig. 7m) and observed an upregulation of *Adrb3* mRNA expression in ingWAT and epiWAT, but not in heart. To analyze whether this regulation could be connected to the DMR pattern that suggested an alteration in neurogenesis-related genes, we analyzed tyrosine hydroxylase (TH) expression in iBAT from P-CE and Ctrl offspring and found that it was increased at both RT and after 2 d of CE in the P-CE offspring (Supplementary Fig. 8a); we also observed higher TH-immunostaining in neuronal axons within the iBAT of the P-CE offspring (Supplementary Fig. 8b,c). We checked vascularization by staining with isolectin B4 (IB4) and found that the iBAT from P-CE offspring was enriched with blood vessels (Supplementary Fig. 8d,e). These data suggested that the iBAT from P-CE offspring was more densely innervated and vascularized, which could explain the hyperactive state.

To test this hypothesis at a functional level, we performed microdialysis of the iBAT from P-CE and Ctrl offspring. We observed an increased release of norepinephrine in P-CE offspring in response to a cold stimulus (Supplementary Fig. 8f). Furthermore, when we blocked adrenergic signaling *in vivo*, either with the selective ADRB3 antagonist L748,337 or the nonspecific  $\beta$ -blocker propranolol before CE, we observed that similar to BAT ablation, pretreatment with L748,337 or propranolol blocked the effect of P-CE on OCR (Supplementary Fig. 8g,h). Taken together, these data demonstrated that P-CE led to higher neuronal innervation and norepinephrine release in the iBAT of P-CE-derived offspring, whereas blocking  $\beta$ -adrenergic receptor signaling in general, or ADRB3 in particular, abrogated the effect of P-CE.

## Discussion

Paternal adaptation to environmental cues have been linked to various physiological changes in the offspring using different animal model systems<sup>22,29</sup>. Our data indicate that CE can be a determinant of the offspring's physiology. This finding is consistent with a recent study suggesting that seasonality can affect systemic metabolism<sup>23,30–33</sup> and that temperature-sensing might influence physiological adaptation. A possible implication for clinical weight-loss studies could be randomization stratified by birth season; however, such a mechanism would have to be investigated in a prospective

trial. Furthermore, despite the large number of individuals studied in our cohort and the low *P* value, our results still need to be interpreted with caution. First, the retrospective nature of the study and the inclusion of individuals undergoing FDG-PET/CT introduces numerous biases. Because BAT was not specifically stimulated, an unknown proportion of 'BAT<sup>-</sup>'-labeled individuals may still have functional but inactive BAT. Second, the location of birth and conception are unknown, which is problematic as there were at least two major immigration waves to Switzerland from southern parts of Europe in the past century<sup>34</sup>. Third, the climate in Switzerland varies substantially and ranges from a mild, Mediterranean-like climate to arctic conditions. Moreover, the clothing style of individuals may not always correlate with the absolute outside temperature, but rather with the perceived meteorological season. Lastly, the amount of daylight has been shown to negatively correlate with BAT activation<sup>35</sup>, and it is an inseparable confounder in this kind of retrospective cohort study.

On the basis of our data we propose that preconception CE of male mice leads to a higher degree of inducibility of brown fat, which is consistent with previous work demonstrating that seminal plasma can be the carrier for phenotypic alterations<sup>36</sup>. A possible explanation for the lack of transmission via the maternal lineage is the anatomical location of testis, which is directly exposed to changes in temperature<sup>37</sup>. Nevertheless, it remains unclear whether sperm directly senses temperature or whether the effect is due to a signal derived from other cells. Although *de novo* methylation is initiated at ~E13.5 in mitotically arrested prospermatogonia, and the methylome is completely established before birth, *de novo* methylation is not initiated until after birth in the female germline. As a result, the sperm methylome is dependent on faithful DNA methylation maintenance, whereas the oocyte methylome is purely reflective of *de novo* methylation events. Furthermore, it should be noted that CE does generally not have the capacity to promote genetic mutations; therefore, the observed phenomenon is not driven by genetic inheritance but by (environmental) epigenetic inheritance.

The observed relative increase in basal brown fat UCP1 protein expression at RT in P-CE offspring might be due to the fact that 23°C constitutes a mild cold challenge to mice<sup>38</sup>. The observed reduction in circulating TAGs is consistent with a previous report demonstrating that BAT is a major sink for TAGs<sup>39</sup>, whereas the higher NEFA levels during fasting in P-CE versus Ctrl mice could be due to enhanced ADRB3 signaling in WAT.

Multiple studies have implicated that BAT has an important role in metabolism; however, very few studies have quantified the actual contribution of BAT. Because *Ucp1* deletion requires breeding and housing at TN, use of *Ucp1*-knockout mice might influence the physiological response<sup>40</sup>. By using an acute model of DTA-targeted ablation exclusive to brown and active brite adipocytes<sup>25</sup>, we were able to show that BAT, at least in part, mediated the observed metabolic changes, even though changes in heart and white fat, or in inflammatory responses, could account for parts of the metabolic alterations.

On the basis of our results, we propose that paternal cold induces a hyperactive state in the BAT of the offspring, which leads to improved adaptation to overnutrition and hypothermia. Various DMRs did overlap with, or were in close proximity to, genes annotated for neurogenesis. Furthermore, the observed denser neuronal innervation, higher vascularization and increased norepinephrine release in iBAT<sup>41</sup> highlighted that multiple genes contributed to this complex phenotype. Together these results suggest the CE affects the sperm methylome, raising the possibility that altered sperm DNA methylation in cold-exposed fathers contributes to the observed phenotype. It is worth noting that this is, to our knowledge, the first example in which adult CE leads to significant alterations in sperm methylation. Although recent studies have shown that 'epivariation', i.e., stochastic individual differences in DNA methylation,

can be the major contributor to the sperm methylome<sup>42</sup>, we would like to point out that the significant concordant global methylation changes, as well as the clear separation of promoter methylation profiles in the sperm of P-CE mice versus that in Ctrl animals, suggest a direct effect of CE on the sperm methylome. Nonetheless, whether these modifications are causative or whether other epigenetic modifications that can convey inherited traits<sup>43</sup>, such as histone modifications<sup>44</sup> or long noncoding and small RNAs<sup>45</sup>, contribute to the observed phenotype remains to be analyzed.

The phenomenon identified here may also have implications for evolutionary biology, as adaptation to environmental temperature changes is critical for any organism. Intergenerational memory of past CEs may have been one mechanism to improve the survival of the offspring during prolonged phases of CE, such as in the ice age 2.6 million years ago. In conclusion, through modulation of genetic and epigenetic variances, environmental changes might influence adipose tissue and metabolism not only in the exposed individual but also in the next generation. Such mechanisms might be exploitable to design therapies and personalized strategies to induce BAT functionality to counteract obesity and comorbidity diseases.

## Methods

Methods, including statements of data availability and any associated accession codes and references, are available at <https://doi.org/10.1038/s41591-018-0102-y>.

Received: 23 November 2017; Accepted: 21 May 2018;

Published online: 9 July 2018

## References

- World Health Organization. Obesity and overweight. Retrieved 22 June, 2018 <http://www.who.int/news-room/fact-sheets/detail/obesity-and-overweight> (2017).
- Rosen, E. D. & Spiegelman, B. M. What we talk about when we talk about fat. *Cell* **156**, 20–44 (2014).
- Tseng, Y. H., Cypess, A. M. & Kahn, C. R. Cellular bioenergetics as a target for obesity therapy. *Nat. Rev. Drug Discov.* **9**, 465–482 (2010).
- Frontini, A. & Cinti, S. Distribution and development of brown adipocytes in the murine and human adipose organ. *Cell Metab.* **11**, 253–256 (2010).
- Bartelt, A. & Heeren, J. Adipose tissue browning and metabolic health. *Nat. Rev. Endocrinol.* **10**, 24–36 (2014).
- Cannon, B. & Nedergaard, J. Brown adipose tissue: function and physiological significance. *Physiol. Rev.* **84**, 277–359 (2004).
- Rosenwald, M. & Wolfrum, C. The origin and definition of brite versus white and classical brown adipocytes. *Adipocyte* **3**, 4–9 (2014).
- Hany, T. F. et al. Brown adipose tissue: a factor to consider in symmetrical tracer uptake in the neck and upper chest region. *Eur. J. Nucl. Med. Mol. Imaging* **29**, 1393–1398 (2002).
- Cypess, A. M. et al. Identification and importance of brown adipose tissue in adult humans. *N. Engl. J. Med.* **360**, 1509–1517 (2009).
- Saito, M. et al. High incidence of metabolically active brown adipose tissue in healthy adult humans: effects of cold exposure and adiposity. *Diabetes* **58**, 1526–1531 (2009).
- van Marken Lichtenbelt, W. D. et al. Cold-activated brown adipose tissue in healthy men. *N. Engl. J. Med.* **360**, 1500–1508 (2009).
- Virtanen, K. A. et al. Functional brown adipose tissue in healthy adults. *N. Engl. J. Med.* **360**, 1518–1525 (2009).
- Zingaretti, M. C. et al. The presence of UCP1 demonstrates that metabolically active adipose tissue in the neck of adult humans truly represents brown adipose tissue. *FASEB J.* **23**, 3113–3120 (2009).
- Nedergaard, J., Bengtsson, T. & Cannon, B. Unexpected evidence for active brown adipose tissue in adult humans. *Am. J. Physiol. Endocrinol. Metab.* **293**, E444–E452 (2007).
- Cypess, A. M. et al. Activation of human brown adipose tissue by a  $\beta$ 3-adrenergic receptor agonist. *Cell Metab.* **21**, 33–38 (2015).
- Yoneshiro, T. et al. Recruited brown adipose tissue as an anti-obesity agent in humans. *J. Clin. Invest.* **123**, 3404–3408 (2013).
- Carone, B. R. et al. Paternally induced transgenerational environmental reprogramming of metabolic gene expression in mammals. *Cell* **143**, 1084–1096 (2010).
- Ng, S. F. et al. Chronic high-fat diet in fathers programs beta cell dysfunction in female rat offspring. *Nature* **467**, 963–966 (2010).
- Jaenisch, R. & Bird, A. Epigenetic regulation of gene expression: how the genome integrates intrinsic and environmental signals. *Nat. Genet.* **33**, 245–254 (2003).
- Seong, K. H., Li, D., Shimizu, H., Nakamura, R. & Ishii, S. Inheritance of stress-induced, ATP-2-dependent epigenetic change. *Cell* **145**, 1049–1061 (2011).
- Anderson, L. M. et al. Preconceptional fasting of fathers alters serum glucose in offspring of mice. *Nutrition* **22**, 327–331 (2006).
- Ng, S. F. et al. Paternal high-fat diet consumption induces common changes in the transcriptomes of retroperitoneal adipose and pancreatic islet tissues in female rat offspring. *FASEB J.* **28**, 1830–1841 (2014).
- Phillips, D. I. & Young, J. B. Birth weight, climate at birth and the risk of obesity in adult life. *Int. J. Obes. Relat. Metab. Disord.* **24**, 281–287 (2000).
- Kaufman, M. H. *The Atlas of Mouse Development* (Academic Press, London, 1994).
- Rosenwald, M., Perdikari, A., Rüllicke, T. & Wolfrum, C. Bidirectional interconversion of brite and white adipocytes. *Nat. Cell Biol.* **15**, 659–667 (2013).
- Hondares, E. et al. Thermogenic activation induces FGF21 expression and release in brown adipose tissue. *J. Biol. Chem.* **286**, 12983–12990 (2011).
- Jones, P. A. Functions of DNA methylation: islands, start sites, gene bodies and beyond. *Nat. Rev. Genet.* **13**, 484–492 (2012).
- Yang, X. et al. Gene body methylation can alter gene expression and is a therapeutic target in cancer. *Cancer Cell* **26**, 577–590 (2014).
- Öst, A. et al. Paternal diet defines offspring chromatin state and intergenerational obesity. *Cell* **159**, 1352–1364 (2014).
- Ly, J. et al. The associations of month of birth with body mass index, waist circumference and leg length: findings from the China Kadoorie Biobank of 0.5 million adults. *J. Epidemiol.* **25**, 221–230 (2015).
- Speakman, J. R. & Heidari-Bakavoli, S. Type 2 diabetes, but not obesity, prevalence is positively associated with ambient temperature. *Sci. Rep.* **6**, 30409 (2016).
- Valdés, S. et al. Ambient temperature and prevalence of obesity in the Spanish population: The Di@bet.es study. *Obes. (Silver Spring)* **22**, 2328–2332 (2014).
- Yang, H. K. et al. Ambient temperature and prevalence of obesity: a nationwide population-based study in Korea. *PLoS One* **10**, e0141724 (2015).
- Afonso, A. Immigration and its impacts in Switzerland. *Mediterranean Quarterly* (Duke University Press) **15**(4), 147–166 (2004).
- Au-Yong, I. T. H., Thorn, N., Ganatra, R., Perkins, A. C. & Symonds, M. E. Brown adipose tissue and seasonal variation in humans. *Diabetes* **58**, 2583–2587 (2009).
- Adefuyi, A. O., Sales, K. J. & Katz, A. A. Seminal plasma induces the expression of IL-1 $\alpha$  in normal and neoplastic cervical cells via EP2-EGFR-PI3K-AKT pathway. *J. Mol. Signal.* **9**, 8 (2014).
- Zhang, Z. et al. Functional analysis of the cooled rat testis. *J. Androl.* **25**, 57–68 (2004).
- Fischer, A. W., Cannon, B. & Nedergaard, J. Optimal housing temperatures for mice to mimic the thermal environment of humans: an experimental study. *Mol. Metab.* **7**, 161–170 (2018).
- Bartelt, A. et al. Brown adipose tissue activity controls triglyceride clearance. *Nat. Med.* **17**, 200–205 (2011).
- Shabalina, I. G. et al. UCP1 in brite (beige) adipose tissue mitochondria is functionally thermogenic. *Cell Rep.* **5**, 1196–1203 (2013).
- Bronnikov, G., Houstek, J. & Nedergaard, J.  $\beta$ -adrenergic, cAMP-mediated stimulation of proliferation of brown fat cells in primary culture. Mediation via  $\beta$ 1- but not via  $\beta$ 3-adrenoceptors. *J. Biol. Chem.* **267**, 2006–2013 (1992).
- Shea, J. M. et al. Genetic and epigenetic variation, but not diet, shape the sperm methylome. *Dev. Cell* **35**, 750–758 (2015).
- Rando, O. J. Intergenerational transfer of epigenetic information in sperm. *Cold Spring Harb. Perspect. Med.* **6**, a022988 (2016).
- Greer, E. L. & Shi, Y. Histone methylation: a dynamic mark in health, disease and inheritance. *Nat. Rev. Genet.* **13**, 343–357 (2012).
- Daxinger, L. & Whitelaw, E. Understanding transgenerational epigenetic inheritance via the gametes in mammals. *Nat. Rev. Genet.* **13**, 153–162 (2012).

## Acknowledgements

We are grateful to M. Stoffel, J. Krützfeldt and members of the Wolfrum lab for helpful discussions, K. Tabbada for assistance with WGBS high-throughput sequencing, and F. Krueger and S. Andrews for help with bioinformatics analysis. We thank K. De Bock and F. Zheng for the IB4 antibody and K. A. Rollins for editing the manuscript. Data produced and analyzed in this paper were generated in collaboration with the Genetic Diversity Center (GDC) and Functional Genomics Center Zurich (FGCZ). The work was supported by the Swiss National Science Foundation (SNSF; C.W. and F.v.M.).

## Author contributions

W.S. and C.W. designed the study; W.S. and H.D. performed all of the experimental work, except that described below; P.P. performed the IVF; S.M. helped with the Seahorse experiments; D.H.D. characterized the Ucp1-DTR-GFP mice; C.W., V.E., M.B. and D.H.D. contributed to the tracing of radiolabeled glucose; E.K. did paraffin sectioning; G.G. quantified lipid droplet sizes; A.P. helped with FACS; V.E. performed automated image analysis; L.G.S. helped with indirect calorimetry analysis; G.S. helped in the

analysis of maternal behavior; D.P.-R. and W.S. did the microdialysis studies; A.S.B., I.A.B., S.B. and C.Z. performed the retrospective analysis of BAT in humans; L.O. contributed to RNA-seq data analysis; F.v.M. and W.R. did DNA methylation sequencing and bioinformatic analysis; W.S. and C.W. wrote the manuscript; and F.v.M., A.S.B., I.A.B., D.H.D., S.M., M.B. and L.B. helped with the editing of the manuscript.

### Competing interests

The authors declare no competing interests.

### Additional information

**Supplementary information** is available for this paper at <https://doi.org/10.1038/s41591-018-0102-y>.

**Reprints and permissions information** is available at [www.nature.com/reprints](http://www.nature.com/reprints).

**Correspondence and requests for materials** should be addressed to C.W.

**Publisher's note:** Springer Nature remains neutral with regard to jurisdictional claims in published maps and institutional affiliations.

## Methods

**Materials.** Details of the reagents used in this study are listed in Life Sciences Reporting Summary.

**Human study.** 13,502 FDG-PET/CT scans of 8,440 individuals that were examined during November to February in the years 2007–2015 were reviewed for the presence of active BAT by physicians<sup>66</sup>. Uptake in the supraclavicular and cervical area was considered to be grade 1, that in the paravertebral and mediastinal areas were considered to be grade 2 and that in the infradiaphragmal area was considered to be grade 3. Readers were blinded to the hypothesis of this study. The birth dates of the individuals were extracted from the 'digital imaging and communications in medicine' (DICOM) metadata of the images. Density plots of the birthdays were created with ggplot2 2.1.0 in R 3.3.1. (R Foundation for Statistical Computing, Vienna, Austria). The distributions of individuals were examined with a generalized linear model (Poisson error distribution and link function) to estimate the likelihood of being conceived in the cold period of the year. The BAT-negative control cohort was matched for sex and age with the nearest-neighbor algorithm<sup>67</sup>. The mean temperature of northern Switzerland was acquired from the Federal Office of Meteorology and Climatology MeteoSuisse in a monthly resolution. The study was approved by the Cantonal Ethics Committee Zürich.

**Mice.** Wild-type C57BL/6N mice were obtained from Charles River Laboratories. Ucp1-DTR-GFP mice were generated as described previously<sup>25</sup>. Unless indicated otherwise, all experiments were performed with adult male mice kept on an inverted 12-h:12-h dark:light cycle, fed ad libitum with a chow diet or a 60% HFD. For cold stimulation, animals were housed in long type II cages at 8°C. All animal studies were approved by the Veterinäramt Zürich.

**Culture of primary adipocytes and HEK 293 cells.** For cellular separation, dissected adipose tissues were minced with a scalpel blade and incubated in 2.0 ml per mg wet tissue 0.2% collagenase type II in collagenase buffer (25 mM KHCO<sub>3</sub>, 12 mM KH<sub>2</sub>PO<sub>4</sub>, 1.2 mM MgSO<sub>4</sub>, 4.8 mM KCl, 120 NaCl, 1.2 mM CaCl<sub>2</sub>, 5 mM glucose, 2.5% BSA, 1% penicillin–streptomycin, pH 7.4) for 50 min at 37°C with occasional resuspension. 10 ml centrifugation buffer (70% PBS, 15% FBS, 15% HistoPaque 1119) was added, and samples were centrifuged for 5 min at 200 g. The SVF pellet from the initial centrifugation was resuspended in 2 ml erythrocyte lysis buffer (154 mM NH<sub>4</sub>Cl, 10 mM KHCO<sub>3</sub>, 0.1 mM EDTA, pH 7.4) and incubated for 4 min on ice. Samples were filtered through 40-µm cell strainers and then centrifuged for 5 min at 200 g. The supernatant was removed, and the pellets were resuspended in culture medium (10% FBS and 1% P/S in DMEM); SVF cells were plated in a plate that was precoated with collagen I and differentiated as described previously<sup>68</sup>. Cells were re-fed every 48 h with 1 µM rosiglitazone and 0.5 µg/ml insulin. Fully differentiated adipocytes were stimulated with CL-316,243 (10 nM) at day 8 (iBAT).

The human HEK293A cell line (Invitrogen) was grown at 37°C, 5% CO<sub>2</sub> in Dulbecco's modified Eagle's medium (DMEM) supplemented with 10% FBS and 1% penicillin–streptomycin. All cells in culture were routinely screened for mycoplasma contamination.

**In vitro fertilization (IVF).** Spermatozoa isolated from cold-treated and control males were used to fertilize oocytes isolated from superovulated C57BL/6 females. The 4-week-old females were superovulated by i.p. administration of 5 IU of equine chorionic gonadotropin (PMSG) and 5 IU of human chorionic gonadotropin (hCG). Males were euthanized, and the dense sperm were isolated from the cauda epididymis and capacitated in 200 µl of Fertip medium (Cosmo Bio) for 45 min at 37°C and 5% CO<sub>2</sub>. Following sperm capacitation, 2 µl of sperm solution was added to the IVF drop, which consisted of 100 µl HTF medium (Cosmo Bio) overlaid with embryo-tested mineral oil (Sigma). The oviducts were immediately dissected, and the oocyte clutches were released into the IVF drop. The IVF reaction was performed for 4 h at 37°C and 5% CO<sub>2</sub>. Following the IVF procedure, oocytes were washed several times in M16 medium, and the efficiency of fertilization was ascertained by the appearance of the pronuclei and the second polar body. Fertilized oocytes were surgically transferred into pseudo-pregnant CD1 foster females that had previously been mated with genetically vasectomized Prnm1GFP males<sup>69</sup>.

**Body composition measurement.** Body composition was measured with the EchoMRI 130 instrument (Body Composition Analyzer, Echo Medical Systems). Mice were fasted for 4 h before measurement.

**Indirect calorimetry.** Indirect calorimetry measurements were performed with the Phenomaster (TSE Systems) according to the manufacturer's guidelines and protocols. Mice were single-caged and acclimated to the metabolic cages for 48 h before metabolic recording.

**Surface temperature measurement.** Surface temperature was recorded with an infrared camera (E60; FLIR; West Malling, Kent, UK) and analyzed with FLIR-Tools-Software (FLIR; West Malling, Kent, UK)<sup>50</sup>.

**Tracing of radiolabeled glucose.** Radiolabeled glucose uptake in tissue was measured as described previously<sup>51</sup>. Mice were fasted for 4 h, then [<sup>14</sup>C]-2-deoxyglucose at 8 mM, 14.8 MBq per kg body weight (MBq/kg) was injected by tail vein. 30 min after injection, blood samples were collected, and mice were euthanized by cervical dislocation. iBAT, epiWAT, ingWAT, liver, skeletal muscle, heart and the brain were dissected, weighed and lysed in 10 volumes of 0.5 M NaOH. Radioactivity was measured by liquid scintillation counting (100 µl of lysate in 3.9 ml of Emulsifier-Safe, Perkin Elmer).

**Insulin tolerance test (ITT).** Mice were fasted for 4 h (chow diet) or 6 h (HFD). Blood was collected from a small incision in the tip of the tail (time 0) and then at 15, 30, 60 and 120 min after an i.p. injection of insulin at 0.6 and 0.75 U per kg body weight for chow-fed and HFD-fed mice, respectively (Actrapid Penfill, Novo Nordisk). Blood glucose levels were measured with a blood glucometer (Accu-Chek Aviva, Roche).

**Behavioral studies.** Maternal behavior quantification was carried out as previously reported<sup>52</sup>. 9-week-old virgin female mice were bred with 9-week-old RT or P-CE male mice. All pregnant females were single-caged, and behavior was recorded throughout the period of pregnancy and nursing by cameras. Maternal nursing behavior was quantified from delivery to postnatal day 11, based on the video recordings.

**Biochemical analysis of plasma.** Mice were fasted for 6 h before euthanization. Blood samples were obtained from cardiac puncture, and plasma was collected after centrifugation for 15 min at 3,000 r.p.m. at 4°C. Cholesterol and triglycerides were measured by enzymatic tests (Roche Diagnostics). Plasma FGF21 levels were analyzed by using the Mouse/Rat FGF-21 ELISA kit (BioVendor). Plasma insulin levels were measured by the Mouse/Rat insulin kit (Meso Scale Discovery). Plasma samples for measuring fasting and refeeding NEFAs was obtained after 12 h of fasting and 4 h of refeeding, by a commercial NEFAs kit (WAKO).

**DNA isolation from sperm and adipose tissue.** DNA from sperm and adipose tissue was extracted with the QIAamp DNA Mini Kit (Qiagen). Sperm samples were isolated from the cauda epididymis and resuspended in M2 medium (Sigma) for 45 min at 37°C. Supernatant containing sperm without tissue debris was collected, pelleted (10,000 g), washed with washing buffer (150 mM NaCl, 10 mM EDTA pH 8.0) and centrifuged for 10 min at 4,000 r.p.m. The sperm pellet was resuspended in 300 µl lysis buffer (100 mM Tris-Cl pH 8.0, 10 mM EDTA, 500 mM NaCl, 1% SDS, 2% β-mercaptoethanol).

**DNA pyrosequencing.** 500 ng DNA (from sperm, adipose tissues or HEK cells) was bisulfite-converted with the EpiTect Bisulfite Kit (Qiagen) according to the manufacturer's protocol. 20 ng of this bisulfite-converted DNA was PCR-amplified with the PyroMark PCR Kit (Qiagen). PCR amplification and sequencing primers (reverse primers were biotinylated) were designed using the Pyromark Assay Design v2.0 software (Qiagen). The quality of the PCR products was checked by gel electrophoresis. Pyrosequencing was applied on a PyroMark Q96 ID using PyroMark Reagents (Qiagen). DNA methylation frequency was quantified with the PyroMark software (Qiagen). Specific CpG sites are illustrated in Supplementary Table 3.

**In vitro methylation assay.** DNA encoding the sequence of mouse *Adrb3* was ordered from Genscript and cloned into pCpGfree-mcs vector (Invivogen). HEK293 cells, with 80% confluency in 24-well plates, were transfected with 1,000 ng/well of either methylated or unmethylated constructs with PEI (Polysciences), at a 4:1 ratio to DNA. 24 h after transfection, medium was replaced. Transfected cells were harvested for analysis 48 h after transfection.

**Tissue harvest.** Mice were euthanized singly in a CO<sub>2</sub> atmosphere. Popliteal lymph nodes were removed from inguinal depots for analyses of gene expression and for cellular separations. Blood was collected by cardiac puncture, and serum was obtained by centrifuging coagulated blood at 10,000 g for 5 min at 4°C.

**Analysis of adipocyte differentiation.** Differentiated adipocytes at day 8 were used for differentiation analysis. Briefly, cells in a 96-well optical plate were fixed with 5% formaldehyde at 4°C for 10 min, followed by three washes with PBS. Cells were stained with LD540 (100 ng/µl) for lipid droplets<sup>53</sup> and Hoechst no. 33342 (100 ng/µl). For UCP1 staining, lipids were depleted by treatment with 5% acetic acid in ethanol for 10 min at -20°C, and cells were washed with PBS twice at RT and blocked in 0.05% Triton X-100 and 5% BSA in PBS. Cells were incubated with a UCP1-specific antibody (1:500; Thermo Fisher PA1-24894) overnight, washed thrice in PBS, incubated with Alexa-Fluor-488-conjugated anti-rabbit-IgG (1:500) secondary antibody and DAPI (to stain nuclei), followed by three washing steps. 29 images per well were taken with an automated microscope imaging system (Operetta, Perkin Elmer). Images were analyzed using the Operetta imaging software as described previously<sup>54</sup>.

**Histology and image analysis.** Adipose tissues were excised, fixed in fresh 4% paraformaldehyde (Sigma) in PBS (Gibco; pH 7.4) for 24 h at 4°C and



then embedded with paraffin. 4- $\mu$ m-thick paraffin sections were subjected to histological staining<sup>55</sup>. Heat-induced antigen retrieval was applied on rehydrated paraffin sections. After blocking with 5% BSA for 1 h, primary antibody (1:200 anti-UCP1; Thermo Fisher) diluted in 5% BSA was applied to sections overnight at 4 °C. After washing with PBS, a secondary antibody (Signal Stain Boost IHC, Cell Signaling) was applied according to Cell Signaling's manual, the sections were washed three times, and the signals were detected using the DAB method (Cell Signaling). Standard H&E staining was performed on rehydrated fat-paraffin sections. Slides were dehydrated and covered with coverslip by resin-based mounting. Analysis of lipid droplet sizes was performed using ImageJ. For each treatment, 21–33 pictures were analyzed. Approximately 18,000–58,000 lipid droplet objects per mouse were used for the computation of lipid droplet size. Oil red O staining was applied on liver cryosections, as previously described<sup>49</sup>. Liver samples were excised, fixed with paraformaldehyde, dehydrated with 30% sucrose and embedded in OCT (Thermo 6502). 10- $\mu$ m-thick sections were cut and stained with freshly prepared ORO (Sigma O0625) staining solution. All images were acquired by an AxioScope A.1 instrument. Representative images were selected in a blinded fashion.

**Fluorescence immunostaining of adipose cryosections.** BAT from Ctrl and P-CE mice were excised and fixed in fresh 4% paraformaldehyde (Sigma-Aldrich) in PBS (Gibco) at pH 7.4 for 2 h at 4 °C, washed four times in PBS and cryopreserved for 30 h in 30% sucrose in PBS with stirring at 4 °C. The samples were flash-frozen on dry ice and stored at –80 °C. BAT samples were cut at –25 °C on an HM 500 O microtome (Microm) at 20- $\mu$ m thickness, mounted on Superfrost plus slides (Mediate), thawed at 4 °C, blocked with 10% donkey serum in PBS for 1 h, and treated with a TH-specific antibody (1:200 in PBS) overnight. Sections were washed three times in PBS at RT, stained with Alexa-Fluor-488-conjugated anti-rabbit-IgG secondary antibody and 300 nM DAPI for 1 h. Slides were embedded in ProLong Diamond Antifade Mountant (Thermo Scientific). Fluorescence micrographs were acquired on an SP5 confocal microscope (Leica). Background was adjusted by using samples without primary antibody.

**Extracellular respiration.** Primary brown preadipocytes were counted and plated at a density of 20,000 cells per well of a Seahorse plate and differentiated to confluence. At day 8 post-differentiation induction, mature brown adipocytes were loaded to an XF<sub>2</sub>, Extracellular Flux Analyzer (Seahorse Bioscience), with one injection of CL-316,243 (10 nM).

**RNA extraction, cDNA synthesis and quantitative RT-PCR.** Total RNA was extracted from tissues or cells using Trizol reagent (Invitrogen) according to the manufacturer's instructions. Reverse transcription was performed to generate a cDNA library by using the High Capacity cDNA Reverse transcription kit (Applied Biosystems), with 1  $\mu$ g of RNA. Quantitative PCR was performed on a ViiA7 instrument (Applied Biosystems), and relative mRNA concentrations, normalized to the expression of *Rplp0* (also known as *36B4*), were calculated by the  $\Delta\Delta C_t$  method. Primer sequences are listed in Supplementary Table 4.

**RNA sequencing (RNA-seq), mapping and analysis.** RNA from BAT was quality-checked by a TapeStation instrument (GE). All samples had a RNA integrity number (RIN) > 8. The rRNA was depleted, and purified RNA was used for the preparation of libraries using the TruSeq RNA sample preparation kit (Illumina), and the samples were sequenced on a HiSeq 4000 HT instrument. RNA-seq sequences were trimmed using Trim Galor (v0.4.4, [http://www.bioinformatics.babraham.ac.uk/projects/trim\\_galore/](http://www.bioinformatics.babraham.ac.uk/projects/trim_galore/)) and mapped to the mouse GRCh38 genome assemblies using hisat2 (v2.1.0). Transcripts were defined using the Ensemble annotations over protein-coding mRNAs. Differential expression analysis of mapped RNA-seq data was performed using DESeq2<sup>57</sup> and EdgeR. Significantly different transcripts were called with significance < 0.05 after Benjamini and Hochberg correction and minimum mean differential expression of twofold. Further analysis was performed using SeqMonk software (<http://www.bioinformatics.babraham.ac.uk/projects/seqmonk/>). Quantitation of RPM values was performed by using the SeqMonk RNA-seq pipeline quantitation on merged transcripts counting reads over exons, correcting for DNA contamination, and log<sub>2</sub>-transformation assuming an opposing strand-specific library transformed by percentile normalization using 'Add' to the 75.0 percentile. Gene ontology (GO) analysis was performed using the gprofiler software (<http://biit.cs.ut.ee/gprofiler/>). Expressed genes were defined where at least one of all four groups (CTRL-3CE, CTRL-RT, P-CE-3CE and P-CE-RT) had a log<sub>2</sub>(RPM) value > 0. Transcriptional similarities between the different samples were computed on all expressed genes using hierarchical clustering (R hclust package) with Euclidian distances and by applying the Ward distance function and plotted as a dendrogram. PCA was performed using the R pcomp package with default parameters.

**Whole-genome bisulfite sequencing (WGBS) mapping and analysis.** Genomic sperm DNA was isolated as described and used for WGBS libraries<sup>58</sup>. Briefly, WGBS libraries were prepared by sonication 500 ng genomic DNA with a Covaris Sonicator into 300- to 400-bp-long fragments, followed by end repair, A-tailing and methylated adaptor (Illumina) ligation using NEB-Next reagents. Libraries

were bisulfite treated using the EZ DNA Methylation-Direct Kit (Zymo), followed by library amplification with indexed primers using KAPA HiFi Uracil + HotStart DNA Polymerase (Roche). All amplified libraries were purified with AMPure XP beads (Agencourt) and assessed for quality and quantity by using High-Sensitivity DNA chips (Agilent Bioanalyzer). High-throughput sequencing of all libraries was performed with a 125-bp paired-end protocol on a HiSeq 2000 instrument (Illumina). Raw sequence reads from WGBS libraries were trimmed to remove poor-quality reads and adaptor contamination, using Trim Galore (v0.4.4, [http://www.bioinformatics.babraham.ac.uk/projects/trim\\_galore/](http://www.bioinformatics.babraham.ac.uk/projects/trim_galore/)). The remaining sequences were mapped using Bismark (v0.18.0)<sup>59</sup> with default parameters to the mouse reference genome GRCh38 in paired-end mode. Reads were deduplicated, and CpG methylation calls were extracted from the deduplicated mapping output using the Bismark methylation extractor (v0.18.0) in paired-end mode. CpG methylation calls were analyzed using R and SeqMonk software (<http://www.bioinformatics.babraham.ac.uk/projects/seqmonk/>). The genome was divided into consecutive probes that had overlapping 50 CpGs each, and the percentage methylation was calculated with the bisulfite feature methylation pipeline in SeqMonk. Global CpG methylation levels were illustrated by using box whisker plots, and promoter methylation similarities between the samples were assessed by using hierarchical clustering (R hclust with Pearson distances and Ward distance function) and PCA (R pcomp package with default parameters). CGI methylation levels were calculated using the SeqMonk bisulfite feature methylation pipeline and averaged over all CpG islands for illustrations. DMRs were calculated using the SeqMonk binomial filter on probes (50 CpG probes or CGIs) with significance < 0.05 after multiple-testing correction and a minimum difference of 10%. GO analysis was performed using the gprofiler software (<http://biit.cs.ut.ee/gprofiler/>) with genes that either overlapped with DMRs or were up to 2 kb downstream of the DMR. DMRs were divided into 'hypermethylated' or 'hypomethylated' in the paternal CE versus control samples. The expression levels of transcripts overlapping with DMRs (logistic regression filter; see above) either hypermethylated or hypomethylated in the BAT samples from P-CE versus Ctrl mice was computed using the log<sub>2</sub>(RPM) gene expression levels in Ctrl BAT samples.

**Western blot analysis.** Protein samples were isolated from adipose tissue with RIPA buffer (50 mM Tris-HCl pH (7.5), 150 mM NaCl, 1 mM EDTA, 1% Triton X-100, 0.1% SDS and 10% glycerol) supplemented with protease inhibitor cocktail (Roche) and Halt phosphatase inhibitor (Thermo Scientific). Homogenized protein lysates were obtained by rotation at 4 °C for 30 min, followed by centrifugation at 14,000 r.p.m. for 30 min. Protein amounts were quantified using the DC Protein Assay (Bio-Rad). For immunoblotting, protein samples were separated by SDS-PAGE on 12% polyacrylamide gels and transferred onto nitrocellulose membrane. Membranes were probed using the indicated antibodies, and chemiluminescent signals were detected by a LAS 4000 mini Image Quant system (GE Healthcare). Band intensity was quantified using ImageJ. Uncropped full scan blots are shown in Supplementary Figs. 9–11.

**In vivo microdialysis from iBAT.** For measuring the release of norepinephrine from iBAT, a microdialysis probe was implanted subcutaneously on the back of the mouse 1 h before the start of the experiment (CMA 20 custom-made, 3-mm membrane, cutoff 20,000 kDa; CMA, Sweden). The microdialysis probe was connected to a pump that flushed artificial cerebrospinal fluid (147 mM Na<sup>+</sup>, 2.4 mM Ca<sup>2+</sup>, 4 mM K<sup>+</sup>, 155.6 mM Cl<sup>-</sup>, pH 6.0) through the probe at a flow rate of 1.5  $\mu$ l/min. The tube was connected to the mouse via a movable arm to allow free movement. After stabilization, samples were collected at 30-min intervals through a refrigerated fraction sampler (MAB 85, Microbiotech AB, Sweden). After baseline samples at RT were collected, temperature was reduced to 8 °C for a period of 3 h.

**Norepinephrine assessment by high-performance liquid chromatography (HPLC).** Dialysate samples from BAT were immediately frozen and stored at –80 °C until injection onto the HPLC (Ultimate 3000, Thermo Scientific, USA) system. Norepinephrine levels were detected and analyzed by using an electrochemical detector (ECD-3000RS, Thermo Scientific, USA) with a coulometric cell (6011RS, Thermo Scientific, USA). The samples were injected via a refrigerated autoinjector (Thermo Fisher, CA, USA) equipped with a 100- $\mu$ l injection loop. Samples were separated on a reversed-phase column (4.6  $\times$  80 mm, 3  $\mu$ m, Thermo Fisher, USA). We used a HPLC pump (ISO-3100BM, Thermo Fisher, USA) and a mobile phase of ammonium acetate, EDTA, 15% methanol and 5% acetonitrile, adjusted to a pH of 6.0, at a flow rate of 0.3 ml/liter at 32 °C. A chromatography workstation (Chromeleon, Thermo Fisher Scientific, Switzerland) was used for data acquisition and calculation.

**Statistical analyses.** For in vivo studies, age-matched male mice were used for all experiments. Sample sizes were determined on the basis of previous experiments using similar methodologies. P-CE and Ctrl fathers always were derived from same litters and were handled in the same manner. One or two offspring were used from each litter for all experiments. The number of litters analyzed for all experiments are indicated in the corresponding figure legends. If more than one mouse from one litter was used, then the mice were analyzed as technical replicates. In total, more than 60 litters per group were analyzed for P-CE and Ctrl mice. Mice were randomly assigned to treatment groups. All of the mice were included for statistical

analyses, and the investigators were not blinded to the mice. RNA and DNA methylation sequencing analyses were blinded to experimental conditions. Results are reported as mean  $\pm$  s.e.m. Two-tailed unpaired Student's *t*-test was applied for comparison. ANOVA was applied on comparisons that involved multiple groups. Statistical differences are indicated as \**P* < 0.05, \*\**P* < 0.01 and \*\*\**P* < 0.001.

**Reporting Summary.** Further information on experimental design is available in the Nature Research Reporting Summary linked to this article.

**Data and software availability.** The Gene Expression Omnibus (GEO) accession number for the WGBS next-generation-sequencing data reported in this study is GSE100231. RNA-seq data were uploaded to European Nucleotide Archive (ENA) with accession number PRJEB15274.

## References


46. Becker, A. S., Nagel, H. W., Wolfrum, C. & Burger, I. A. Anatomical grading for metabolic activity of brown adipose tissue. *PLoS One* **11**, e0149458 (2016).
47. Ho, D. E., Imai, K., King, G. & Stuart, E. A. Matching as nonparametric preprocessing for reducing model dependence in parametric causal inference. *Polit. Anal.* **15**, 199–236 (2007).
48. Kazak, L. et al. A creatine-driven substrate cycle enhances energy expenditure and thermogenesis in beige fat. *Cell* **163**, 643–655 (2015).
49. Haueter, S. et al. Genetic vasectomy–overexpression of PRM1-EGFP fusion protein in elongating spermatids causes dominant male sterility in mice. *Genesis* **48**, 151–160 (2010).
50. Whittle, A. J. et al. BMP8B increases brown adipose tissue thermogenesis through both central and peripheral actions. *Cell* **149**, 871–885 (2012).
51. Abreu-Vieira, G. et al. Cidea improves the metabolic profile through expansion of adipose tissue. *Nat. Commun.* **6**, 7433 (2015).
52. Pryce, C. R., Bettschen, D., Nanz-Bahr, N. I. & Feldon, J. Comparison of the effects of early handling and early deprivation on conditioned stimulus, context and spatial learning and memory in adult rats. *Behav. Neurosci.* **117**, 883–893 (2003).
53. Spandl, J., White, D. J., Peychl, J. & Thiele, C. Live-cell multicolor imaging of lipid droplets with a new dye, LD540. *Traffic* **10**, 1579–1584 (2009).
54. Meissburger, B. et al. Adipogenesis and insulin sensitivity in obesity are regulated by retinoid-related orphan receptor gamma. *EMBO Mol. Med.* **3**, 637–651 (2011).
55. Sanchez-Gurmaches, J. & Guertin, D. A. Adipocytes arise from multiple lineages that are heterogeneously and dynamically distributed. *Nat. Commun.* **5**, 4099 (2014).
56. Mehlem, A., Hagberg, C. E., Muhl, L., Eriksson, U. & Falkevall, A. Imaging of neutral lipids by oil red O for analyzing the metabolic status in health and disease. *Nat. Protoc.* **8**, 1149–1154 (2013).
57. Love, M. I., Huber, W. & Anders, S. Moderated estimation of fold change and dispersion for RNA-seq data with DESeq2. *Genome Biol.* **15**, 550 (2014).
58. von Meyenn, F. et al. Comparative principles of dna methylation reprogramming during human and mouse in vitro primordial germ-cell specification. *Dev. Cell* **39**, 104–115 (2016).
59. Krueger, F. & Andrews, S. R. Bismark: a flexible aligner and methylation caller for bisulfite-seq applications. *Bioinformatics* **27**, 1571–1572 (2011).

RESEARCH

Open Access



# Sperm DNA methylation epimutation biomarker for paternal offspring autism susceptibility

Nicolás Garrido<sup>1</sup>, Fabio Cruz<sup>1</sup>, Rocio Rivera Egea<sup>1</sup>, Carlos Simon<sup>2,3</sup>, Ingrid Sadler-Riggelman<sup>4</sup>, Daniel Beck<sup>4</sup>, Eric Nilsson<sup>4</sup>, Millissia Ben Maamar<sup>4</sup> and Michael K. Skinner<sup>4\*</sup> 

## Abstract

**Background:** Autism spectrum disorder (ASD) has increased over tenfold over the past several decades and appears predominantly associated with paternal transmission. Although genetics is anticipated to be a component of ASD etiology, environmental epigenetics is now also thought to be an important factor. Epigenetic alterations, such as DNA methylation, have been correlated with ASD. The current study was designed to identify a DNA methylation signature in sperm as a potential biomarker to identify paternal offspring autism susceptibility.

**Methods and results:** Sperm samples were obtained from fathers that have children with or without autism, and the sperm then assessed for alterations in DNA methylation. A genome-wide analysis (> 90%) for differential DNA methylation regions (DMRs) was used to identify DMRs in the sperm of fathers ( $n = 13$ ) with autistic children in comparison with those ( $n = 13$ ) without ASD children. The 805 DMR genomic features such as chromosomal location, CpG density and length of the DMRs were characterized. Genes associated with the DMRs were identified and found to be linked to previously known ASD genes, as well as other neurobiology-related genes. The potential sperm DMR biomarkers/diagnostic was validated with blinded test sets ( $n = 8-10$ ) of individuals with an approximately 90% accuracy.

**Conclusions:** Observations demonstrate a highly significant set of 805 DMRs in sperm that can potentially act as a biomarker for paternal offspring autism susceptibility. Ancestral or early-life paternal exposures that alter germline epigenetics are anticipated to be a molecular component of ASD etiology.

**Keywords:** Autism, Sperm, Epigenetics, Diagnostic, Generational, Father, Offspring

## Introduction

Autism spectrum disorder (ASD) is a complex neurological disorder involving deficits in communication, social behaviors and stereotypic movements [1, 2]. The prevalence of ASD in 1975 was reported as 1 in 5000 and then in 2009 as 1 in 110 [3]. The American Centers for Disease Control and Prevention reported a 1 in 88 prevalence in 2012 and then a 1 in 68 in 2014. Although improved

diagnosis and current awareness have played a role in this increase, particularly in the first couple decades (1975–2000), the increase in the last two decades is thought to be due to environmental and molecular factors [2–4]. This is supported by twin studies and numerous environmental studies. Genetic studies using genome-wide association studies (GWAS) have identified multiple genetic mutations, but they are correlated with only a small percentage of the autism patients [5]. A recent study identified sperm genetic alterations associated with offspring autism [6]. Combining genetic mutations and altered epigenetics appear to improve associations [7]. Many specific toxicants and factors have been suggested

\*Correspondence: skinner@wsu.edu

<sup>4</sup> Center for Reproductive Biology, School of Biological Sciences, Washington State University, Pullman, WA 99164-4236, USA  
Full list of author information is available at the end of the article



© The Author(s) 2021. **Open Access** This article is licensed under a Creative Commons Attribution 4.0 International License, which permits use, sharing, adaptation, distribution and reproduction in any medium or format, as long as you give appropriate credit to the original author(s) and the source, provide a link to the Creative Commons licence, and indicate if changes were made. The images or other third party material in this article are included in the article's Creative Commons licence, unless indicated otherwise in a credit line to the material. If material is not included in the article's Creative Commons licence and your intended use is not permitted by statutory regulation or exceeds the permitted use, you will need to obtain permission directly from the copyright holder. To view a copy of this licence, visit <http://creativecommons.org/licenses/by/4.0/>. The Creative Commons Public Domain Dedication waiver (<http://creativecommons.org/publicdomain/zero/1.0/>) applies to the data made available in this article, unless otherwise stated in a credit line to the data.

to be involved, but generally more extensive analysis is required [8]. Environmental factors are now believed to be involved in the etiology of autism. A number of molecular alterations in the genome have been correlated to the neurobiology of ASD [2]; however, the specific environmental factors, molecular processes and etiology of autism remain to be fully elucidated.

Although there are both paternal and maternal transmission of ASD, the prevalence of paternal transmission is higher in most populations. One of the main factors proposed to be involved is paternal age [9], with an increased percentage risk of 28% between 40–49 years and nearly 70% when greater than 50 years of age [4]. Increased paternal age has been associated with epigenetic DNA methylation alterations in sperm [10], including specific genes associated with autism [11, 12]. Paternal age-associated DNA methylation alterations have been shown to impact offspring health and disease susceptibility [13, 14]. Therefore, the current study controlled for age at conception and sample collection for the comparison. In addition to paternal age effects, ancestral and early-life exposures to toxicants, abnormal nutrition and stress can also impact sperm DNA methylation to potentially affect disease susceptibility of offspring [15]. The current study was designed to examine the father's sperm epigenetics (DNA methylation) in families with or without autistic children. The hypothesis examined is that a father's specific sperm DNA methylation alterations will correlate with offspring autism susceptibility.

Epigenetics is defined as “molecular factors and processes around DNA that regulate genome activity independent of DNA sequence and are mitotically stable.” The molecular factors and processes currently known are DNA methylation, histone modifications, chromatin structural changes, noncoding RNA and RNA methylation [15]. When the epigenetic alterations become programmed in the germ cells (sperm or egg), they have the potential to promote in subsequent generations the epigenetic transgenerational inheritance of disease and phenotypic alterations [15]. Environmental factors that promote these early-life epigenetic alterations have the ability to promote epigenetic inheritance to subsequent generations and dramatically increase disease susceptibility and prevalence [15–17]. The current study was designed to use an epigenome-wide association study approach and develop a potential paternal sperm biomarker for offspring autism susceptibility.

The use of specific sperm epigenetic (DNA methylation) alterations (i.e., biomarkers) could be used for a fathers (i.e., paternal) offspring autism susceptibility, and applications in an assisted reproduction setting could be considered. Although genetic tests are common in assisted reproduction and preimplantation diagnostics,

epigenetic analysis is less common. Sperm DNA methylation diagnostics have been proposed for the use in assisted reproduction [18]. The availability of a sperm DNA methylation biomarker for offspring autism susceptibility would allow improved clinical management and early treatment options to be considered. An epigenome-wide association study for DNA methylation alterations in sperm from fathers with or without autistic children was used to identify potential sperm epigenetic alterations as a biomarker for paternal offspring autism susceptibility.

## Results

Paternal males with children affected by autism (case) or without (control) were recruited, and paternal sperm samples were collected at the Andrology Laboratory of IVIRMA Clinic in Valencia, Spain. The sperm sample was collected upon enrollment. Thirty-six patients were enrolled, which included thirteen in the control group, thirteen in the autism case group, and eight or ten for the blinded test groups. The differences (mean  $\pm$  SD) between the semen analysis for both control and case group are shown in Table 1. Observations from the groups showed no significant difference in age, fathers age at pregnancy, fathers age upon sperm collection, sperm volume, concentration, or sperm concentration between the groups. Progressive sperm motility was greater in the autism case group, with no difference in non-progressive sperm motility, as shown in Table 1a. The motile percentage was higher in the control group, and no difference was observed in the total motile sperm count. One of the control samples, IVI 14, had a very high sperm count of 396.62 million that was outside two standard deviations of the mean ( $2 \pm$  SD), so the analysis was redone without this sample. When the IVI 14 sample was not used in the analysis, the total sperm number was increased in the autism case group ( $p < 0.02$ ), and the total motile sperm count (time) was increased in the autism case group ( $p < 0.017$ ), as well as the progressive spermatozoa (%) ( $p < 0.019$ ) and immotile % ( $p < 0.019$ ) parameters. In addition to the case and control male age and sperm analysis parameters, Table 1a, all the blinded test set males, Table 1b, c, age and sperm parameters were analyzed and found to also be within the mean  $\pm$  SD of the case and control samples presented (Additional file 2: Figure S1). Therefore, the blinded test set of individuals was appropriate comparisons with the same clinical parameters.

The participant demographics and clinical information were similar between the case and control population participants. The ethnicity of all the fathers was Caucasian. No major comorbidities were observed within either the control or case populations. The date

**Table 1 Sperm samples and clinical semen analysis.**

Study sample	Paternal sperm analysis												
	Sample	Age (years)	Father age (years) upon collection	Father age (years) at pregnancy	Collection date of sample	Offspring autism case/control	Volume (mL)	Concentration (mill/mL)	Total of spermatozoa (mill)	Progressive spermatozoa (%)	Non-progressive spermatozoa (%)	Immotile (%)	Total motile sperm count (time)
(a) Sperm samples and clinical analysis													
MI1	42	42	31	31	7/27/15	Case	2.2	83	182.6	58	11	31	105.91
MI2	44	45	43	43	7/28/15	Case	1.5	38	57	42	11	47	23.94
MI3	41	41	38	38	7/29/15	Case	3	68	204	44	11	45	89.76
MI4	38	38	34	34	7/29/15	Case	3.4	66	224.4	35	11	54	78.54
MI5	37	37	33	33	7/30/15	Case	1.4	10	14	50	14	36	7
MI6	39	49	40	40	8/4/15	Case	2.2	23	50.6	31	26	43	15.69
MI7	41	41	31	31	8/12/15	Case	6	47	282	69	14	17	194.58
MI8	42	42	32	32	8/14/15	Case	2.5	91	227.5	60	15	25	136.5
MI9	45	45	35	35	9/9/15	Case	3.5	87	304.5	50	13	37	152.25
MI10	-	39	31	31	9/28/15	Case	3	33.3	99.9	44	9	47	43.96
MI11	-	45	39	39	12/21/15	Case	4	120	480	50	12	38	240
MI12	35	37	24	24	9/5/17	Case	5.4	36.3	196.02	43	3	54	84.29
MI13	46	46	35	35	3/7/16	Case	4.2	17.6	73.92	60	17	23	44.35
MI14	40	40	36	36	10/11/16	Control	2.8	141.65	396.62	55	10	35	218.14
MI15	41	41	36	36	10/11/16	Control	1	34.3	34.3	31	18	51	10.63
MI16	46	46	35	35	10/17/16	Control	2.2	5.5	12.1	29	3	68	3.51
MI17	44	44	33	33	10/20/16	Control	4.8	10.5	50.4	42	12	46	21.17
MI18	38	38	31	31	10/21/16	Control	3.2	1.6	5.12	28	13	59	1.43
MI19	36	36	34	34	11/3/16	Control	6.8	14	95.2	32	3	65	30.46
MI20	41	41	41	41	3/22/17	Control	2.2	91.8	201.96	49	14	37	98.96
MI21	42	42	32	32	5/23/17	Control	1.4	42.1	58.94	37	23	40	21.81
MI22	37	37	29	29	9/6/17	Control	4.2	54	226.8	52	9	39	117.94
MI23	43	43	36	36	9/6/17	Control	1.8	13	23.4	23	20	57	5.38
MI24	54	54	27	27	9/15/17	Control	2.5	52	130	48	7	45	62.4
MI25	38	38	34	34	9/15/17	Control	5.5	1.7	9.35	11	8	81	1.03
MI26	43	43	33	33	9/22/17	Control	1.5	96	144	35	17	48	50.4
Mean ± SD	41 ± 3	42 ± 4	34 ± 5	34 ± 5	Offspring autism case		3 ± 1	55 ± 33	184 ± 128	49 ± 11	13 ± 5	38 ± 12	94 ± 71
Mean ± SD	42 ± 5	42 ± 5	34 ± 3	34 ± 3	Offspring control		3 ± 2	43 ± 44	107 ± 114	36 ± 13	12 ± 6	52 ± 14	49 ± 63
Statistical comparison	NS	NS	NS	NS	(Case vs. Control), not significant (NS) > 0.05		NS	NS	NS	p < 0.01	NS	p < 0.01	NS

**Table 1 (continued)**

<b>(b) Blinded test sample set 1 analysis</b>		
BS 1	Identified case	Actual case
BS 2	Identified control	Actual control
BS 3	Identified control	Actual control
BS 4*	Identified control	Actual Case*
BS 5	Identified case	Actual case
BS 6	Identified case	Actual case
BS 7	Identified control	Actual control
BS 8	Identified control	Actual control
<b>(c) IVI blinded test sample set 2 analysis</b>		
BS 9	Identified case	Actual case
BS 10	Identified case	Actual case
BS 11	Identified case	Actual case
BS 12	Identified case	Actual case
BS 13	Identified control	Actual control
BS 14*	Identified control	Actual case*
BS 15	Identified control	Actual control
BS 16	Identified control	Actual control
BS 17	Identified control	Actual control
BS 18	Identified control	Actual control

(a) The samples were provided by IVI-RMA, Valencia, Spain, that collected and performed the clinical analysis of semen volume, sperm concentration and analysis, motility and formal progression analysis, and motility analysis. The mean  $\pm$  SD for case and control samples is provided. A Student's *t* test was used to assess any statistical differences between case and control groups. (b) Blinded test sample set #1 analysis. The analysis was performed to identify the case or control samples and then confirmed once completed after analysis unblinded. (c) Blinded test sample set #2 analysis. IVI-RMA provided an additional ten blinded samples, and following analysis (Identified) was unblinded to assess accuracy (Actual). The false-negative identifications are indicated with an (\*) on the labels



of the patient sperm collection, age of the father upon collection and age of the father at conception of child are all not statistically different and provided in Table 1. Although age can impact sperm DNA methylation, the mean age upon sperm collection, which required a 3-year collection period, for the case and control was not statistically different, as given in Table 1. In addition, no statistical difference was observed in the age of the fathers at conception of child, as given in Table 1. All the autistic children were males. Since the focus was on paternal sperm, and due to IRB restrictions, the offspring ASD spectrum severity was not considered. The human subjects approval and informed consent were obtained from all participants prior to the initiation of the study and approved by the Ethics Committee of Valencian Infertility Institute—Reproductive Medicine Associates (IVIRMA) Valencia, Spain, with code, #1311-VLC-136-FC.

Individual patient sperm samples from the collection upon enrollment were prepared for sperm analysis, and an aliquot was taken and flash frozen with liquid nitrogen and stored at  $-20^{\circ}\text{C}$  until shipment on dry ice for the epigenetic analysis. The samples were thawed, and prior to DNA isolation, the sperm were sonicated to destroy and remove any contaminating somatic cells, as previously described [16]. Due to the sperm nuclei being resistant to sonication, any contaminating somatic cells are removed following sonication. The DNA was extracted from the sperm and then fragmented for a methylated DNA immunoprecipitation (MeDIP) procedure to obtain methylated DNA for analysis to identify differential DNA methylated regions (DMRs). The MeDIP is a genome-wide analysis examining 95% of the genome, which is comprised of low-density CpG regions in comparison with the less than 5% of the genome of high-density CpG regions such as CpG islands. The MeDIP DNA libraries were prepared for next-generation DNA sequencing by creating individual patient sequencing libraries. Samples were then sequenced for bioinformatic analysis, as described in Additional file 1 section. A comparison of the sequences between the control (non-autism children) and case (autism children) participant sperm samples identified DMRs, as shown in Fig. 1a. At a  $p$  value of  $p < 1e-05$  there were 805 DMRs identified with the majority being a single 1-kb window with fewer (i.e., six) having multiple adjacent 1-kb windows involved. The DMRs at a number of  $p$  values are presented for  $p < 001$  to  $p < 1e-07$ , Fig. 1a. The DMRs at EdgeR  $p < 1e-05$  all had false discovery rate (FDR) of  $p < 0.05$  and were used for subsequent data analysis. The  $p < 1e-05$  was used to optimize DMR numbers and statistical considerations. A list of these DMRs with various genomic features (e.g., CpG density and chromosomal location) are presented in Additional file 3: Table S1. Observations suggest that

males with autistic children have a sperm DMR signature that is distinct from males without autistic children (control).

The genomic features of the offspring autism susceptibility DMRs were investigated. The chromosomal locations of the DMRs at  $p < 1e-05$  within the human genome are presented in Fig. 1b. The red arrowheads indicate the individual DMRs, and the black boxes represent clusters of DMRs. The DMRs are present on all chromosomes. The CpG density of the DMRs is generally less than 10 CpG per 100 bp with 1–3 CpG predominant for the paternal offspring autism susceptibility DMRs, as shown in Fig. 1c. The size of the DMRs was predominantly 1–3 kb for the sperm DMRs, as shown in Fig. 1d. Additional genomic features are presented in Additional file 4: Table S1. The log-fold change (LFC) in DNA methylation in Additional file 3: Table S1 demonstrated for the 805 DMR in the autism group that 303 have an increase in DNA methylation and 502 have a decrease in DNA methylation. The autism DMRs involved a 38% increase or 62% decrease in DNA methylation. Therefore, the majority of the sperm DMRs had low CpG density, termed a CpG desert, and were 1 kb in length with either an increase or decrease in DNA methylation.

The paternal offspring autism susceptibility sperm DMR-associated genes and corresponding gene functional categories were determined, as presented in Additional file 4: Table S1. The total autism 805 DMRs had 193 with no DMR gene associations (24%), and the DMRs were intergenic and not associated with genes. From the 612 DMR with gene associations (76%), there were 493 DMR that overlapped with annotated genes. There were 17 DMR in the 1–1000 bp and 62 DMR in the 1–5 kb proximal promoter regions. There were 40 DMRs in the 5–10 kb distal promoter region. Therefore, approximately 20% of the DMR are in the proximal and distal promoter region and 80% overlapping the gene annotation regions. There were 193 DMRs that were intergenic. These DMRs are intergenic and not proximal to genes, but can influence gene expression events for megabase distances through ncRNA and chromatin structure alterations, as previously described [19, 20]. Genes within 10 kb of a DMR were identified, which has previously been shown to be optimal for both proximal and distal promoter regions and epigenetic associations [21]. The functional categories corresponding to each DMR-associated gene are summarized in Fig. 2a. The signaling, transcription and metabolism functional categories are predominant. This reflects that these gene functional categories have the highest number of genes within them. A comparison of previously identified genes associated with neurodegeneration, neurodevelopment and autism with the DMR-associated genes of this study is summarized in

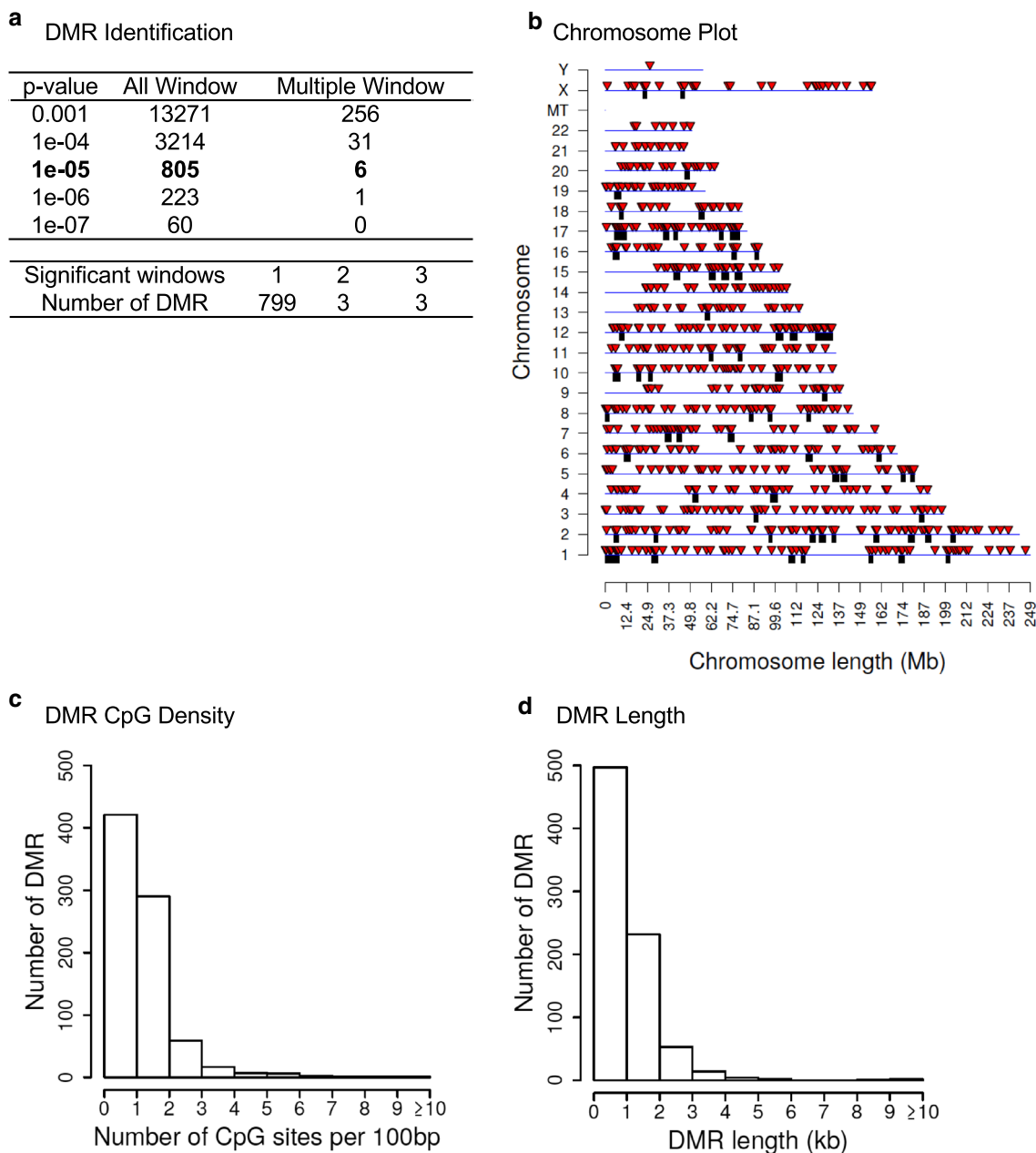


**Fig. 1** **a** DMR identifications. Autism case versus control sperm DMR analysis. The number of DMRs found using different  $p$  value cutoff thresholds. The all window column shows all DMRs. The multiple window column shows the number of DMRs containing at least two adjacent significant windows and the number of DMRs with each specific number of significant windows at a  $p$  value threshold of  $1e-05$ . **b** Autism case versus control patient DMR analysis. The DMR locations on the individual chromosomes are identified. All DMRs at a  $p$  value threshold of  $p < 1e-05$  are shown with the red arrowheads and clusters of DMRs with the black boxes. **c** DMR CpG density in the autism case versus control patient DMRs. The number of DMRs at different CpG densities is indicated. All DMRs at a  $p$  value threshold of  $p < 1e-05$ . **d** Autism case versus control patient DMR lengths in kilobases. All DMRs at a  $p$  value threshold of  $1e-05$  are shown

Fig. 2b. These autism-associated genes have previously been shown to be regulated or involve genetic mutations within autism patients, and the gene symbols, descriptions and associated references are presented in

Additional file 5: Table S2. The DMR-associated genes were also used in a gene pathway or gene set analysis to identify associated pathways. Interestingly, the top pathway or gene set identified was autism, and the majority

(See figure on next page.)

**Fig. 2** **a** DMR-associated gene categories. DMRs at a  $p$  value threshold  $p < 1e-05$  are shown. **b** Autism case versus control DMR PCA. PCA for DMRs at  $p < 1e-05$ . The first two principal components used and samples color code index indicated. The underlying data are the RPKM read depth for all DMRs. **c** DMR-associated genes and autism. The paternal offspring autism-susceptible DMRs previously shown to correlate with autism and associated neurodegenerative disease are presented. DMR-associated genes from the current study were compared to genes associated with autism in the published literature using Pathway Studio software (Elsevier, Inc.). Those that were in common are depicted

of the subsequent pathways with greater than three genes were all neurodevelopmental- or neurobiology-associated pathways, as given in Table 2. All those gene sets were found to be significant, and a list of the specific DMR-associated genes is provided, as given in Table 2. As shown with all the DMR-associated genes, Additional file 5: Table S2, the associated genes in Table 2 also had approximately a 50% mixture of genes with an increase or decrease in DNA methylation. Therefore, the DMR-associated genes did correlate well with previously identified autism- and neurodevelopment-associated genes. Since the sperm DMRs will impact the embryo epigenomes and transcriptomes of all subsequent somatic cells, this dynamic cascade of developmental epigenetics needs to be considered in potential links in sperm epigenetics and potential neurological impacts on autism.

The final analysis examined the statistical significance and validation of the DMRs identified. A permutation analysis was performed on the DMRs to determine whether the DMRs were due to background variation in the data or randomly generated. The permutation analysis shows the number of DMRs generated from the control versus autism case comparison was significantly greater than the DMRs generated from random subset analysis, Additional file 3: Figure S2. The red line to the right indicates the comparison DMRs versus the low numbers from the random subset comparison. Another analysis involved a cross-validation of the DMRs and demonstrated approximately 80% accuracy in the confirmation of the DMRs to assess autism susceptibility [22]. A principal component analysis (PCA) of the control male sperm without an autistic child versus the male sperm with an autistic child is presented in Fig. 2c. A clear separation of the DMR principal components is seen between the groups. This demonstrates a distinction between the DMR principal components.

The final validation involved using blinded test sets of samples for analysis to identify and assess the accuracy to determine actual case or control samples. Three different molecular analyses of the original 13 cases and 13 controls were performed and combined for this test set analysis. The test set analysis involved four independent analyses that were combined for the final analysis. The first test set involved eight blinded samples selected from the main analysis samples and reanalyzed (BS1–BS8) and identified as actual case or control sample, as given

in Table 1b. All were accurately identified, except one false negative which was identified as a control, but actually was a case sample. A second set of ten blinded test samples (BS9–BS18) was provided by IVI-RMA clinical collaborators and was also identified in an independent analysis as case or control, as given in Table 1c. All were accurately identified, except one false negative which was identified as a control, but was actually a case sample. Therefore, the blinded test set analysis indicated all but one in each test set were accurately identified for approximately a 90% accuracy in the analysis. Since multiple analysis was used for this blinded test set analysis, random batch effect outlier DMRs identified were removed to optimize the analysis. Although significantly more validation with larger clinical test sets is needed, the current study provides the proof of concept that epigenetic biomarkers potentially exist and may be used to diagnose that a father may potentially have a child with a susceptibility for autism.

## Discussion

The frequency of autism in the population has dramatically increased over tenfold the past several decades. This increase appears to be due in part to increased diagnosis efficiency from 1975 to the early 2000s, as well as greater public awareness of the disease [3]. The more recent increase in the last couple of decades suggests environmental factors, and exposures also have a critical role in autism prevalence. Although many suggestions have been made on specific toxicants and factors being involved, more extensive analysis and better understanding of autism etiology are needed to understand this increase in autism frequency [8]. An example is the suggestion-assisted reproduction and in vitro fertilization is involved, but follow-up studies demonstrated no risk of ASD in children born after assisted reproduction [23, 24]. One factor that has been correlated with autism is paternal age [4, 9, 15] and sperm DNA methylation alterations [11, 25]. Previous studies have shown a hypermethylation of sperm DNA is associated with male infertility, abnormal sperm parameters and increasing age [13, 26, 27]. Therefore, the majority of DMR involve an increase in DNA methylation when associated with infertility or age. The current study demonstrated 60% of the DMRs have a decrease in DNA methylation, and 40% of DMRs an increase in DNA methylation, Additional file 4: Table S1.

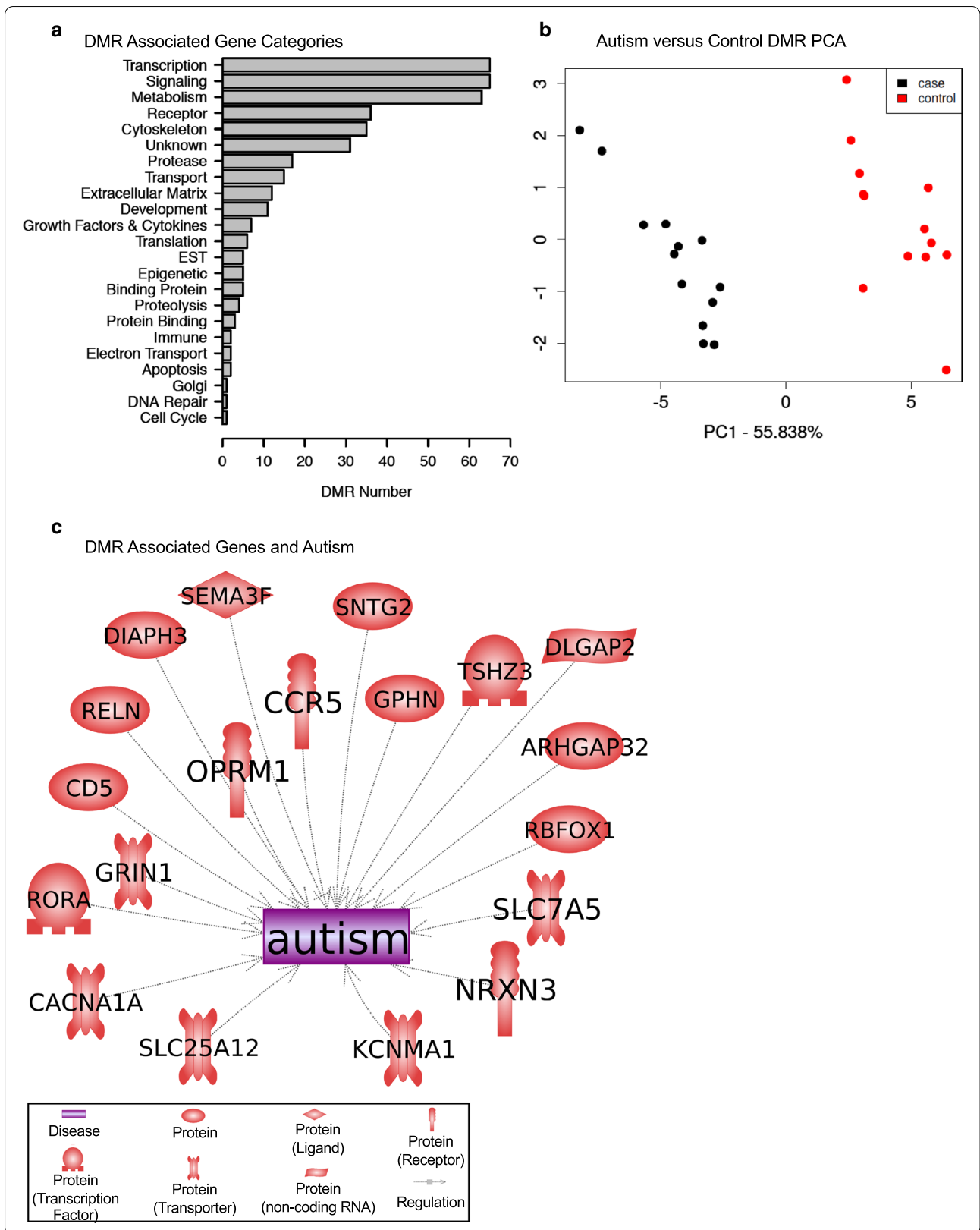


**Table 2 DMR-associated gene pathways or gene sets.**

Pathway or gene set name	Total # of neighbors	Pathology gene set pathway	Overlap	Percent overlap	Overlapping genes	p value
Protein regulators of autism	313	Autism	19	6	RBFOX1, CD5, CCR5, GRIN1, GPHN, SLC7A5, SNTG2, RELN, ARHGAP32, OPRM1, DLGAP2, DIAPH3, CACNA1A, KCNMA1, TSHZ3, SLC25A12, NRXN3, SEMA3F, RORA	9.02E-05
Protein regulators of intellectual disability	616	Intellectual disability	28	4	SRGAP3, ERBB4, DMD, TG, AHI1, ANKRD11, CHL1, ST3GAL5, BCKDK, CDK19, DLGAP2, NARS2, PHF21A, KDM2B, CAMTA1, MCPH1, CREBBP, ARHGEF10, TCF4, LIMK1, STIM1, RELN, PRMT7, DPYSL2, SORL1, LRMDA, CDH18, EXOC4	3.42E-04
Protein regulators of neurodevelopmental disorder	273	Neurodevelopmental disorder	16	5	RBFOX1, SRGAP3, GRIN1, LIMK1, AHI1, DOCK3, ANKS1B, ELP4, ANKRD11, RELN, DPYSL2, ST3GAL5, AGAP1, MCPH1, CREBBP, TCF4	4.70E-04
Protein regulators of psychiatric disorder	538	Psychiatric disorder	25	4	GRIN2B, PDE2A, ERBB4, AHI1, CCKBR, ANKS1B, DLGAP1, CCDC141, OPRM1, PDLIM5, GABBR1, SORCS2, CREBBP, ARHGEF10, TCF4, DNMT1, RBFOX1, GPHN, USP46, RELN, DPYSL2, ADRA2C, IMMP2L, NRXN3, ALK	5.12E-04
Protein regulators of intellectual impairment	18	Intellectual impairment	4	21	GRIN2B, GRIN1, DMD, RELN	5.95E-04
Protein regulators of estrogen receptor-positive breast cancer	86	Estrogen receptor-positive breast cancer	8	9	KDM6B, PPARG, ERBB4, PIK3CD, NDRG1, CREBBP, SLC7A5, STIM1	6.90E-04
Protein regulators of behavioral disorder	147	Behavioral disorder	10	6	GRIN2B, GRIN1, ERBB4, PARK7, STX1A, RORA, DNMT1, TMEM173, AP2B1, OPRM1	1.80E-03
Protein regulators of severe visual impairment	14	Severe visual impairment	3	20	PAX2, APL1, MERTK	3.39E-03

The pathway total number of neighbors for genes, pathology gene set pathway, overlapping genes, percent overlap, overlapping gene symbols and statistical p value are presented

Therefore, a mixture of an increase and decrease in methylation is observed, which is distinct from the sperm hypermethylation observed in male infertility and aging [13, 26, 27]. Since all the paternal subjects were similar in age and fertile (Table 1), the current study observations appear to be distinct from infertility and aging-related DNA hypermethylation. Although some participants from both control and case populations were involved in *in vitro* fertilization upon sperm collection, male factor infertility was not involved. No differences in demographics or clinical variables were observed. The age upon sperm collection between the case and control was not statistically different, as given in Table 1. In addition, the age at conception of child was also not statistically different between case and control participants. The comparison was biased on age of sperm collection to control for age differences to minimize DNA methylation variation. However, similar observations were also obtained considering age of conception of child. Therefore, the current study was designed to identify sperm epigenetic alterations (i.e., biomarkers) to assess a father's potential ability to transmit autism susceptibility to his offspring.

Altered germline epigenetics has been shown to impact offspring health later in life, and if permanently programmed, to promote the epigenetic transgenerational inheritance of disease and pathology to subsequent generations [15, 16]. Since sperm or egg epigenetics can impact the zygote epigenetics and transcription following fertilization, as well as the subsequent stem cell population in the early embryo epigenome and transcriptome, all subsequently derived somatic cells also have the potential to have an altered cell-type specific epigenomes and transcriptomes later in development [15, 28]. This molecular alteration has been shown to be associated with adult somatic cell epigenetics, transcriptomes and associated diseases [29–31]. The ability of an ancestral or early-life exposure to impact the germline epigenetics to subsequently impact the offspring epigenetics and susceptibility to develop pathology and disease has been established [15–17, 28–31] and is anticipated to be a component of autism etiology as well. The current study observations support the concept that similar events may contribute to autism etiology.

The application of a sperm molecular diagnostic is optimally used in an assisted reproduction setting. Routine semen analysis and genetic testing are used in most *in vitro* fertilization clinical settings. Although epigenetic analysis is not as routine, the proposal for such analysis has been made [18]. The analysis of male infertility using sperm DNA methylation alterations has been developed [32]. Epigenetic alterations (DNA methylation) in sperm have been shown to associate in fathers of families with

autistic children [33]. That study used a targeted array-based approach that focused on high-density CpG islands that constitutes approximately 1% of the genome, but does demonstrate such an analysis is feasible. The current study was designed to use a genome-wide approach to identify altered DNA methylation for paternal sperm and offspring autism susceptibility.

Although genetics will be involved in autism etiology, genome-wide association studies (GWAS) have demonstrated generally less than 1% of the patients with a specific disease, such as neurodegenerative disease that has a correlated genetic mutation [34]. ASD is similar to only a few percent correlation with associated genetic mutations [35]. An additional molecular mechanism to consider for ASD disease etiology involves epigenetics. The current study uses a more epigenome-wide association study approach to investigate sperm DNA methylation in fathers with or without autistic children. A procedure to assess DNA methylation alterations in low-density CpG regions, that constitute over 95% of the human genome, was used in comparison with the high-density CpG procedures previously used. A significant signature of differential DNA methylation regions (DMRs) was identified comparing the sperm from fathers with or without autistic children. The genomic features of the DMRs were identified and demonstrated generally 1-kb lengths and low-density CpG regions. The DMR-associated genes were identified, and a number of previously identified autism-linked genes were present (Fig. 2b, Additional file 5: Table S2 and Table 2). In regard to the autism sperm DMR biomarkers, a separation in a principal component analysis (PCA) was observed. In addition to this validation, the permutation and cross-validation analyses help demonstrate the robustness and sensitivity of the analysis. The validation studies with blinded sample sets accurately identified the majority of case and control samples, but potential false-negative identification of case samples was observed. The observations demonstrate the paternal sperm epigenetic analysis is potentially effective at identifying offspring susceptibility for autism, but the current analysis needs to be improved with expanded clinical trials.

Although an epigenetic signature was identified for paternal transmission of susceptibility of autism children, which was identified and statistically significant, a limitation of the current study is the low number of samples used for the analysis. Although epigenetic alterations occur at a significantly higher frequency than genetics, expanded clinical trials are required with increased numbers, greater ethnic diversity, and more thorough assessment of the impacts of paternal age. The impacts of these variables need to be elucidated to improve and expand the accuracy of the analysis.



The expanded clinical trial with greater numbers and diverse subpopulations is essential to develop a useful diagnostic. However, the current study does provide the proof of concept; such a diagnostic can be developed.

Applications of the paternal offspring autism susceptibility biomarker/diagnostic will potentially improve the health care for ASD patients. This would allow IVF patients to assess risk and determine management procedures. Importantly, this would allow clinicians to plan the offspring's clinical management options more efficiently. Potential preventative treatments could be considered to reduce the severity of the autism spectrum disorder. The availability of the assay could also be used in a research setting to facilitate the identification of environmental factors potentially involved in the ASD etiology. Therefore, potential therapeutic and preventative options not previously considered could be taken.

The current study identified a genome-wide signature of DNA methylation sites that are associated with the paternal transmission of offspring autism susceptibility. Although a large clinical trial is needed to further validate the biomarkers and potential diagnostic, the current study provides the proof of concept for the assay and biomarkers. Therefore, the identification of offspring susceptibility can be assessed, allowing better clinical management of ASD. The potential for therapy options can be expanded to improve health care for ASD. Such epigenetic biomarkers are anticipated to exist for many disease and pathology conditions, which will facilitate the future preventative medicine strategies for health care. In addition, the current study suggests epigenetic inheritance may play a role in ASD etiology and explain the paternal transmission prevalence of the disease.

## Methods summary

### Clinical sample collection

A single-center (IVIRMA Valencia, Spain) prospective and open clinical study was performed. The participant approval and informed consent were obtained from all participants prior to the clinical sample collection. The study protocols were approved by the Institutional Review Board Ethics Committee of Valencian Infertility Institute—Reproductive Medicine Associates (IVIRMA) Valencia, Spain, with code, #1311-VLC-136-FC. All research was performed in accordance with relevant guidelines/regulations. The study was not designed for, nor did the IRB involve, the ability to correlate autism child clinical information to be correlated. The semen was analyzed as described in Additional file 1. Samples were immersed in liquid nitrogen and then stored at  $-20^{\circ}\text{C}$  prior to analysis.

### Epigenetic analysis, statistics and bioinformatics

Somatic cell contamination was removed by sonication, and the sperm DNA was isolated as previously described [16]. Methylated DNA immunoprecipitation (MeDIP), followed by next-generation sequencing (MeDIP-Seq), was performed. MeDIP-Seq, sequencing libraries, next-generation sequencing, and bioinformatics analysis were performed as described [16] and are found in Additional file 1. The statistical analysis and validation protocols were performed as previously described [16] and are found in Additional file 1. All molecular data has been deposited into the public database at NCBI (GEO # GSE157417), and R code computational tools are available at GitHub (<https://github.com/skinnerlab/MeDIP-seq>) and [www.skinner.wsu.edu](http://www.skinner.wsu.edu).

### Supplementary Information

The online version contains supplementary material available at <https://doi.org/10.1186/s13148-020-00995-2>.

**Additional file 1:** Supplemental methods.

**Additional file 2: Figure S1.** Clinical group statistic comparison. The various sperm/seminal characteristics in the Study case and control group were compared with the Blind group. The n-value, mean, standard deviation, and standard error mean are presented. The blind groups are within the mean  $\pm$  SD of the case and control study.

**Additional file 3: Figure S2.** Permutation analysis. The number of DMR for autism case versus control patient comparison for all permutation analyses. The vertical red line shows the number of DMR found in the original analysis. All DMRs are defined using an edgeR  $p$  value threshold of  $p < 1e-05$ .

**Additional file 4: Table S1.** DMR lists at  $p < 1e-05$  with presentation of name, chromosomal location, DMR start and stop nucleotide number for chromosome, length (bp), number of 1 kb significant windows, minimum  $p$  value, CpG number and density, DMR maximum, log-fold change (max-LFC) (+ increase DNA methylation and – decrease DNA methylation), and gene association within 10 kb and gene functional categories.

**Additional file 5: Table S2.** Gene and protein regulators of autism. The DMR-associated autism-related genes with symbol, description, and relevant references PubMed ID (PMID) numbers.

### Abbreviations

ASD: Autism spectrum disorder; IVF: In vitro fertilization; DMRs: Differential DNA methylation regions; GWAS: Genome-wide association studies; MeDIP: Methylated DNA immunoprecipitation; MeDIP-Seq: Methylated DNA immunoprecipitation followed by next-generation sequencing; FDR: False discovery rate; LFC: Log-fold change; PCA: Principal component analysis; BS: Blinded samples.

### Acknowledgements

We acknowledge Ms. Jayleana Barton and for technical assistance and all technicians from IVIRMA Andrology Laboratory for assistance in the clinical sample collection. We acknowledge Ms. Amanda Quilty for editing and Ms. Heather Johnson for assistance in preparation of the manuscript. We thank the Genomics Core laboratory at WSU Spokane for sequencing data. We acknowledge Epigenesis Inc., Pullman, WA, where the initial molecular analysis was performed. This study was supported by Epigenesis Inc., Pullman, WA, USA, and John Templeton Foundation (50183 and 61174) (<https://templeton.org/>) grants to MKS. The funders had no role in study design, data collection and analysis, decision to publish, or preparation of the manuscript.

### Authors' contributions

NG performed clinical and sample collection oversight, data analysis and editing manuscript. FC was involved in patient's recruitment and editing manuscript. RRE contributed to patient's recruitment, clinical and sample collection oversight, data analysis and editing manuscript. CS conceived, initiated sample collection and edited the manuscript. ISR was involved in molecular analysis, data analysis and editing manuscript. DB performed bioinformatics, data analysis and editing manuscript. EN done sample processing, data analysis and editing manuscript. MBM was involved in sample processing, molecular analysis, data analysis and editing manuscript. MKS conceived, analyzed the data, performed funding acquisition and wrote the manuscript. All authors read and approved the final manuscript.

### Funding

This study was supported by Epigenesys Inc., Pullman, WA, USA, and John Templeton Foundation (50183and61174) (<https://templeton.org/>) grants to MKS. The funders had no role in study design, data collection and analysis, decision to publish, or preparation of the manuscript.

### Availability of data and materials

All molecular data have been deposited into the public database at NCBI (GEO # GSE157417), and R code computational tools are available at GitHub (<https://github.com/skinnerlab/MeDIP-seq>) and [www.skinner.wsu.edu](http://www.skinner.wsu.edu).

### Ethics approval and consent to participate

The participant approval and informed consent were obtained from all participants prior to the clinical sample collection. The IRB study was approved by the Ethics Committee of Valencian Infertility Institute—Reproductive Medicine Associates (IVIRMA) Valencia, Spain, with code, #1311-VLC-136-FC. All research was performed in accordance with relevant guidelines/regulations.

### Consent for publication

Not applicable.

### Competing interests

The authors report no conflict of interest.

### Author details

<sup>1</sup> IVI-RMA Valencia, and IMI Foundation, Health Research Institute La Fe, Valencia, Spain. <sup>2</sup> Dept Ob/Gyn, Valencia University/Instituto de Investigacion Clinica, Hospital Clinico de Valencia (INCLIVA), and Igenomix Foundation, Valencia, Spain. <sup>3</sup> Beth Israel Deaconess Medical Center, Harvard University, Boston, USA. <sup>4</sup> Center for Reproductive Biology, School of Biological Sciences, Washington State University, Pullman, WA 99164-4236, USA.

Received: 1 July 2020 Accepted: 17 December 2020

Published online: 07 January 2021

### References

- King BH, Navot N, Bernier R, Webb SJ. Update on diagnostic classification in autism. *Curr Opin Psych*. 2014;27(2):105–9.
- Kumar S, Reynolds K, Ji Y, Gu R, Rai S, Zhou CJ. Impaired neurodevelopmental pathways in autism spectrum disorder: a review of signaling mechanisms and crosstalk. *J Neurodev Disord*. 2019;11(1):10.
- Weintraub K. The prevalence puzzle: autism counts. *Nature*. 2011;479(7371):22–4.
- Kimura R, Yoshizaki K, Osumi N. Risk of neurodevelopmental disease by paternal aging: a possible influence of epigenetic alteration in sperm. *Adv Exp Med Biol*. 2018;1012:75–81.
- Autism Spectrum Disorders Working Group of The Psychiatric Genomics Consortium. Meta-analysis of GWAS of over 16,000 individuals with autism spectrum disorder highlights a novel locus at 10q24.32 and a significant overlap with schizophrenia. *Mol Autism*. 2017;8:21.
- Breuss MW, Antaki D, George RD, Kleiber M, James KN, Ball LL, et al. Autism risk in offspring can be assessed through quantification of male sperm mosaicism. *Nat Med*. 2020;26(1):143–50.
- Massrali A, Brunel H, Hannon E, Wong C, Baron-Cohen S, et al. Integrated genetic and methylomic analyses identify shared biology between autism and autistic traits. *Mol Autism*. 2019;10:31.
- Herbert MR. Contributions of the environment and environmentally vulnerable physiology to autism spectrum disorders. *Curr Opin Neurol*. 2010;23(2):103–10.
- Yassin W, Kojima M, Owada K, Kuwabara H, Gonoji W, Aoki Y, et al. Paternal age contribution to brain white matter aberrations in autism spectrum disorder. *Psychiatry Clin Neurosci*. 2019;73(10):649–59.
- Frans EM, Sandin S, Reichenberg A, Langstrom N, Lichtenstein P, McGrath JJ, et al. Autism risk across generations: a population-based study of advancing grandpaternal and paternal age. *JAMA Psych*. 2013;70(5):516–21.
- Atsem S, Reichenbach J, Potabattula R, Dittrich M, Nava C, Depienne C, et al. Paternal age effects on sperm FOXP1 and KCNA7 methylation and transmission into the next generation. *Hum Mol Genet*. 2016;25(22):4996–5005.
- Milekic MH, Xin Y, O'Donnell A, Kumar KK, Bradley-Moore M, Malaspina D, et al. Age-related sperm DNA methylation changes are transmitted to offspring and associated with abnormal behavior and dysregulated gene expression. *Mol Psych*. 2015;20(8):995–1001.
- Jenkins TG, Aston KI, Pflueger C, Cairns BR, Carrell DT. Age-associated sperm DNA methylation alterations: possible implications in offspring disease susceptibility. *PLoS Genet*. 2014;10(7):e1004458.
- Rumbold AR, Sevoyan A, Oswald TK, Fernandez RC, Davies MJ, Moore VM. Impact of male factor infertility on offspring health and development. *Fertil Steril*. 2019;111(6):1047–53.
- Nilsson E, Sadler-Riggelman I, Skinner MK. Environmentally induced epigenetic transgenerational inheritance of disease. *Environ Epigenet*. 2018;4(2):1–13.
- King SE, McBirney M, Beck D, Sadler-Riggelman I, Nilsson E, Skinner MK. Sperm epimutation biomarkers of obesity and pathologies following DDT induced epigenetic transgenerational inheritance of disease. *Environ Epigenet*. 2019;5(2):1–15.
- Anway MD, Cupp AS, Uzumcu M, Skinner MK. Epigenetic transgenerational actions of endocrine disruptors and male fertility. *Science*. 2005;308(5727):1466–9.
- Simon L, Emery BR, Carrell DT. Review: diagnosis and impact of sperm DNA alterations in assisted reproduction. *Best Pract Res Clin Obstet Gynaecol*. 2017;44:38–56.
- Haque MM, Nilsson EE, Holder LB, Skinner MK. Genomic Clustering of differential DNA methylated regions (epimutations) associated with the epigenetic transgenerational inheritance of disease and phenotypic variation. *BMC Genom*. 2016;17(418):1–13.
- Skinner MK, Manikkam M, Haque MM, Zhang B, Savenkova M. Epigenetic transgenerational inheritance of somatic transcriptomes and epigenetic control regions. *Genome Biol*. 2012;13(10):R91.
- Lehman DA, Patterson B, Johnston LA, Balzer T, Britton JS, Saint R, et al. Cis-regulatory elements of the mitotic regulator, *string/Cdc25*. *Development*. 1999;126(9):1793–803.
- Hastie T, Tibshirani R, Friedman J. The elements of statistical learning: data mining, inference, and prediction. 2nd ed. New York: Springer; 2009.
- Hvidtjorn D, Grove J, Schendel D, Schieve LA, Svaerke C, Ernst E, et al. Risk of autism spectrum disorders in children born after assisted conception: a population-based follow-up study. *J Epidemiol Commun Health*. 2011;65(6):497–502.
- Sandin S, Nygren KG, Iliadou A, Hultman CM, Reichenberg A. Autism and mental retardation among offspring born after in vitro fertilization. *JAMA*. 2013;310(1):75–84.
- Siu MT, Weksberg R. Epigenetics of autism spectrum disorder. *Adv Exp Med Biol*. 2017;978:63–90.
- Laqqan M, Solomayer EF, Hammadeh M. Aberrations in sperm DNA methylation patterns are associated with abnormalities in semen parameters of subfertile males. *Reprod Biol*. 2017;17(3):246–51.
- Alkhaled Y, Laqqan M, Tierling S, Lo Porto C, Hammadeh ME. DNA methylation level of spermatozoa from subfertile and proven fertile and its relation to standard sperm parameters. *Andrologia*. 2018;50(6):e13011.
- Jirtle RL, Skinner MK. Environmental epigenomics and disease susceptibility. *Nat Rev Genet*. 2007;8(4):253–62.
- Guerrero-Bosagna C, Savenkova M, Haque MM, Nilsson E, Skinner MK. Environmentally induced epigenetic transgenerational inheritance of altered sertoli cell transcriptome and epigenome: molecular etiology of male infertility. *PLoS ONE*. 2013;8(3):1–12.

30. Nilsson E, Klukovich R, Sadler-Riggleman I, Beck D, Xie Y, Yan W, et al. Environmental toxicant induced epigenetic transgenerational inheritance of ovarian pathology and granulosa cell epigenome and transcriptome alterations: ancestral origins of polycystic ovarian syndrome and primary ovarian insufficiency. *Epigenetics*. 2018;13(8):875–95.
31. Klukovich R, Nilsson E, Sadler-Riggleman I, Beck D, Xie Y, Yan W, et al. Environmental toxicant induced epigenetic transgenerational inheritance of prostate pathology and stromal-epithelial cell epigenome and transcriptome alterations: ancestral origins of prostate disease. *Sci Rep*. 2019;9(2209):1–17.
32. Aston KI, Uren PJ, Jenkins TG, Horsager A, Cairns BR, Smith AD, et al. Aberrant sperm DNA methylation predicts male fertility status and embryo quality. *Fertil Steril*. 2015;104(6):1388–97.
33. Feinberg JL, Bakulski KM, Jaffe AE, Tryggvadottir R, Brown SC, Goldman LR, et al. Paternal sperm DNA methylation associated with early signs of autism risk in an autism-enriched cohort. *Int J Epidemiol*. 2015;44(4):1199–210.
34. Visscher PM, Brown MA, McCarthy MI, Yang J. Five years of GWAS discovery. *Am J Hum Genet*. 2012;90(1):7–24.
35. Kim YS, Leventhal BL. Genetic epidemiology and insights into interactive genetic and environmental effects in autism spectrum disorders. *Biol Psychiat*. 2015;77(1):66–74.

### Publisher's Note

Springer Nature remains neutral with regard to jurisdictional claims in published maps and institutional affiliations.

**Ready to submit your research? Choose BMC and benefit from:**

- fast, convenient online submission
- thorough peer review by experienced researchers in your field
- rapid publication on acceptance
- support for research data, including large and complex data types
- gold Open Access which fosters wider collaboration and increased citations
- maximum visibility for your research: over 100M website views per year

**At BMC, research is always in progress.**

Learn more [biomedcentral.com/submissions](https://biomedcentral.com/submissions)

